ABSTRACT

The development of a dynamic, mechanistic model of the ozone/peroxide destruction of a micropollutant is discussed. A mathematical model consisting of a set of partial differential and algebraic equations to describe the change in concentration in a bubble contactor for each species is presented, and numerical methods to solve this system of equations are discussed briefly. Sensitivity of the model to input parameters is investigated; particularly, the reaction rate constant between the micropollutant and the hydroxyl radical, mass transfer coefficient, liquid dispersion coefficient, gas dispersion coefficient, influent pH, total carbonate species concentration, and reactor configuration. Transient results show the system approaches steady state within three bed-volumes under the specified conditions. Model predictions indicate that in the presence of carbonate species, the rate constant between the micropollutant and the hydroxyl radical is of particular importance for micropollutant removal. Species having rate constants greater than 10^9 $M^{-1}s^{-1}$ compete well with the carbonate/hydroxyl radical reactions. Results demonstrate the efficiency of micropollutant removal in low dispersion reactors. Gas phase dispersion and reactor configuration are shown to have relatively little effect on predicted micropollutant removal. Model predictions compare well to data from an existing ozone/peroxide plant.

ACKNOWLEDGMENTS

Many thanks to my advisor, Dr. Glaze, for the opportunity to pursue this research and for his guidance. Thanks also to Dr. Miller for helping me develop my knowledge of numerical methods and for his involvement in this work. Thanks to Dr. Aitken for joining the others on my committee. Thanks to Dr. Joseph Pedit, who knows the truth is out there, wrote the code to find it, and provided the Lyle Lovett background music. Thanks to Ed Hill and Phil Weeber for sharing their knowledge of UNIX and love of sock puppets. Thanks to my research group for stimulating, thought-provoking conversations, and for other conversations which were blessedly neither. Thanks to my office-mates Howard Weinberg, Sue Homewood and Rob Haith (the king of the smoke break) for not throwing me out whenever I visited the deep end. Special thanks to Sue and Matt for housing during the end. My sincere appreciation to the manufacturers of caffeinated beverages, particularly Main Street Espresso whose 12 oz cappuccino has sustained me for the last few weeks. Thanks to Mom and Dad for the erector set when I was very young, to all of my family and friends for their support, and to my husband Jon, who loves me with or without this degree.

Support for this work was provided by the Army Environmental Policy Institute.

TABLE OF CONTENTS

LIST OF TABLES

LIST OF ILLUSTRATIONS

LIST OF ABBREVIATIONS

ADR: Advective Dispersive Reactive
AOP: Advanced Oxidation Processes
BDF: Backward Difference Formula
CSTR: Completely Stirred Tank Reactor
D: Direct Reactors with Hydroxyl Radical
DAE: Differential Algebraic Equation
E_o: Standard Oxidation Potential
FDM: Finite Difference Method
FEM: Finite Element Method
GAC: Granular Activated Carbon
I: Initiators for Decomposition of Ozone
LADWP: Los Angeles Department of Water and Power
M: Molar
M_i: Micropollutant
MOL: Method of Lines
NHE: Standard Hydrogen Electrode
NOM: Natural Organic Matter
ODE: Ordinary Differential Equation
P: Promoter of Decomposition of Ozone
PCE: Perchloroethylene
PDE: Partial Differential Equation
s: seconds
S_i: Scavenger of Hydroxyl Radical
TOC: Total Organic Carbon
U.S.: United States
UNC-CH: University of North Carolina Chapel Hill
UV: Ultraviolet light

LIST OF SYMBOLS

Ψ: scavenging capacity of water

Γ: source/sink term

υ_α: velocity of phase α

ΔV: volume increment

θ_w: volume fraction of water

$[HO^{\cdot}]_{SS}$: steady state concentration of hydroxyl radical

$[O_3]^*$: liquid interface ozone concentration

$C_{i,\alpha}$: concentration of species i in phase α

$CO_3^{\cdot-}$: carbonate radical

CO_3^{2-}: carbonate ion

D_α: dispersion coefficient in phase α

e^-: aqueous electron

H^+: hydrogen ion

H_2CO_3: carbonic acid

H_2O: water

H_2O_2: hydrogen peroxide

HCO_3^-: bicarbonate ion

H_i: Henry's law constant for species i

h_L: liquid phase holdup

$HO^{\cdot}$: hydroxyl radical

$HO_2^{\cdot}$: hydroperoxyl radical

K_a: acidity equilibrium constant

$k^F_{HA,A}$: forward reaction for equilibrium constant between HA and A^-

k_La: overall mass transfer coefficient

$k_{M,N}$: reaction rate constant between species M and N

$k^R_{HA,A}$: reverse reaction for equilibrium constant between HA and A^-

O_2: oxygen

$O_2^{\cdot}$: superoxide anion

O_3: ozone

OH^-: hydroxide ion

P: partial pressure

pH: negative log of hydrogen ion concentration

pK: negative log of equilibrium constant

Q_G: gas phase flow rate

Q_L: liquid phase flow rate

r_m: degradation rate of micropollutant

w: specific ozone utilization rate

1. INTRODUCTION

1.1 Advanced Oxidation Processes

The hydroxyl radical ($HO^{\cdot}$) is a highly reactive species which can be used for the oxidation of micropollutants in water. Processes which rely on $HO^{\cdot}$ and other highly reactive radicals for the removal of organic micropollutants are frequently referred to as Advanced Oxidation Processes or AOPs (Glaze et al., 1987). The most widely used AOPs include combinations of ozone (O_3) with ultraviolet light (UV) or hydrogen peroxide (H_2O_2) and photooxidation with H_2O_2. The former rely on the acceleration of the free radical decomposition of O_3 (Hoigne and Bader, 1975) in order to increase the $HO^{\cdot}$ concentration (Aieta et al., 1988). Increasingly, these processes are being considered as alternatives to traditional phase transfer technologies for the treatment of organic contaminated waters and wastewaters (Haas and Vamos, 1995).

The ozone/hydrogen peroxide process (O_3/H_2O_2) uses hydrogen peroxide to accelerate the decomposition of O_3 to form $HO^{\cdot}$. The process is applicable for the oxidation of organic contaminants in industrial wastewater treatment and groundwater remediation, as well as for the control of taste and odor causing compounds and micropollutants in surface water treatment (Glaze et al., 1990). Currently, drinking water ozonation facilities are being built to allow for the easy addition of hydrogen peroxide. By the end of this century, it is estimated that approximately forty to fifty potable water plants with the potential for O_3/H_2O_2 capabilities will be on-line (Rice, 1995).

Commercial and municipal applications of the O_3/H_2O_2 process, as well as other AOPs, have preceded a complete understanding of their chemistry and mechanisms.

Indeed, some practical applications have been implemented without systematic studies of AOPs and their mechanisms, advantages and disadvantages, or comparison to other technologies (Glaze, 1993). Little has been done to thoroughly evaluate AOPs or compare them to traditional technologies.

1.2 Technology Assessment Project Goals

In 1994, a study to develop the necessary tools for the comparison of traditional technologies with more innovative technologies, including AOPs, was initiated at UNC-CH in collaboration with government, academic, and industrial partners. The multi-phase project was designed to evaluate these technologies on a level playing field. This level playing field was to be maintained by specifying the same waste streams, plant scales and economic parameters for comparison. Ranges of plant scales and concentrations were to be used to help identify economies of scale. Phase I of the project was planned to use only model compounds for evaluation. Phase II was designed to proceed into real and complex wastestreams. The end result of the project will be written summaries of technologies which include Phase I and II assessments, as well as models which practitioners can use to conduct their own preliminary evaluations. This will provide a useful tool for the scientific and engineering communities for technology screening.

One goal of the project was to provide models based on the scientific fundamentals which predict performance and costs for each technology. For some traditional technologies (GAC adsorption and air stripping), such models were found to exist. However, since preliminary literature searches demonstrated a lack of comprehensive

models for more advanced technologies (Glaze et al., 1994), it became necessary to develop such models for O_3/H_2O_2 and other AOPs. The work presented in this technical report is part of the effort to develop comprehensive process models for these technologies.

1.3 Modeling Concerns For O_3/H_2O_2

Several items should be considered in the development of an O_3/H_2O_2 process model if it is to be representative of practical applications. It is desirable to have a model which is based on the chemical mechanism behind the process. This allows the model to be used to predict performance for different systems without refitting empirical parameters.

O_3/H_2O_2 reactors in the U.S. are primarily bubble contactors (Marinas et al., 1993), or other types of flow-through reactors. The dispersion model can be used in this case to represent plug flow in the liquid phase disturbed by dispersion due to the bubbles in the column (Marinas et al., 1993). Gas phase flow can also be modeled as plug flow with some dispersion.

Reaction rates are fast, so under some conditions the reactions may be limited by the mass transfer of O_3 from the gas phase into the liquid phase. To accurately predict performance, it is necessary to include the mass transfer term in a model of such systems (Haas and Vamos, 1995).

Additionally, reactor inflow conditions may vary with time, including changes in flow rate or influent concentrations. A transient solution will predict the response of the system to such changes, which may be important for everyday operations of the system.

Several species in the O_3/H_2O_2 system are subject to speciation controlled by pH. The different chemical species react at different rates, therefore it is necessary to include the speciation constants as part of the system of equations describing O_3/H_2O_2 destruction of a micropollutant. These chemical equilibria manifest a series of algebraic constraints for the partial differential equations which describe the concentration changes in the system.

Finally, the accepted mechanism for the oxidation of a micropollutant is not complete: often by-products and their chemistries are unknown. A useful model must be flexible to accommodate the addition of such compounds as the mechanism is better understood. This may lead to the ability to predict the formation of byproducts.

Generally, present models have not met all of these concerns. Early models (Staehelin and Hoigne, 1985; Yurteri, 1988; Glaze and Kang, 1989a) dealt only with batch reactors and steady state solutions. Speciation has been handled by solving only for the steady state solution, after pH controlled speciations have become constant. Recent model developments (Laplanche et al., 1995) still were not designed for transient solutions and included empirical models to describe mixing in the reactors. Additionally, the models do not allow for the easy addition of further mechanistic information, such as byproducts.

1.4 Research Objectives

The objective of this research is to develop a flexible, dynamic, mechanistic model of the O_3/H_2O_2 oxidation of a micropollutant in a plug flow reactor, and to test the sensitivity and logic of the model results. Using this model, the importance of transient solutions for AOP models can be investigated, possibly leading to the simplification of future AOP models.

2. BACKGROUND

2.1 Chemistry of AOPs

As previously mentioned, AOPs rely on the generation of reactive free radicals, particularly $HO^{\cdot}$, to enhance their reactivity (Glaze and Kang, 1989a). This is done in systems utilizing O_3 by accelerating the free radical decomposition of O_3 to increase $HO^{\cdot}$ production. $HO^{\cdot}$ is so powerful and fast a reactant that AOP treatment of most organic substrates can be practical at steady state concentrations of $HO^{\cdot}$ as low as 10^{-10}-10^{-12} M (Glaze and Kang, 1989a).

The reactions involved in the decomposition of aqueous O_3 in pure water are shown in Figure 1. Note that the decomposition of O_3 is initiated only by OH^- in this matrix. The reaction rate constant for the initiation reaction ($k=70\ M^{-1}s^{-}1$) is rather slow. Ozonation at high pH can accelerate this process by increasing OH^- concentration. Also, the process may be accelerated by the reaction of O_3 with superoxide (O_2^-) produced by oxidative degradation of natural organic matter and other organics which may be present in the water source. Note that in pure water $HO^{\cdot}$ reacts with O_3 to form the hydroperoxyl radical (HO_2) which is in equilibrium with superoxide (O_2^-) , and this propagates the chain reaction. Thus O_3 is highly unstable in pure water (Staehelin and Hoigne, 1985).

Figure 1: The Reactions of Ozone in "Pure" Water (Staehelin and Hoigne, 1985)

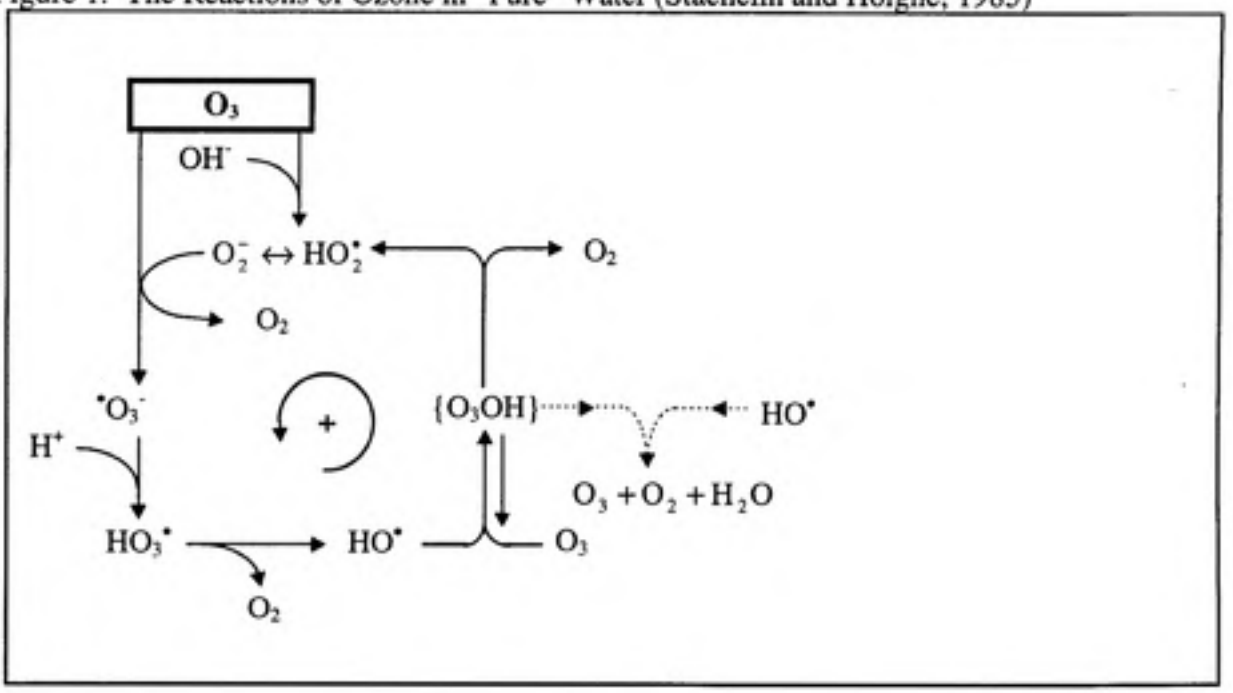

In the case of O_3/H_2O_2, the conjugate base of H_2O_2 can act as an initiator (Staehelin and Hoigne, 1982) in addition to OH^-. The rate constant for Equation 1, k = $5.5 \times 10^6\ M^{-1}s^{-1}$ (Staehelin and Hoigne, 1982), results in a faster rate than for initiation by OH^-, even though it is the conjugate base (HO_2^-) which reacts with O_3.

$$HO_2^- + O_3 \rightarrow HO_2 + O_3^- \qquad (1)$$

Combining O_3 with UV also accelerates the initiation of O_3 decomposition, providing an additional initiation pathway by producing H_2O_2 in situ. The photolysis of O_3 produces oxygen atoms in the ^1D state which can insert rapidly into water to form H_2O_2, as shown in Equations 2a and 2b (Taube, 1957; Peyton and Glaze, 1987,1988).

$$O_3 + h\nu \rightarrow O(^1D) + O_2 \quad (2a)$$

$$O(^1D) + H_2O \rightarrow HO^{\bullet} + O_2 \quad (2b)$$

The conjugate base of H_2O_2 is then available to initiate the decomposition of O_3 as was shown previously in Equation 1.

2.1.1 Chemistry of O_3/H_2O_2

Contaminant removal in the O_3/H_2O_2 system may occur via at least two pathways: direct oxidation by molecular O_3 or oxidation by $HO^{\cdot}$ (Hoigne and Bader, 1975).

Ozone

O_3 has a standard oxidation potential versus the NHE of 2.07 volts (Equation 3), making it much stronger than more conventional oxidants such as chlorine, permanganate or hydrogen peroxide (Haas and V̇amos, 1995).

$$O_3 + 2H^+ + 2e^- \leftrightarrow O_2 + H_2O \quad E_o = 2.07 \text{ V} \quad (3)$$

The practicality of O_3 for the oxidation of contaminants is, however, limited by kinetics. The second order rate constants for several compounds with molecular O_3 are shown in Table 1. It can be seen that these constants vary over several orders of magnitude with some slow enough to preclude the use of molecular O_3 as a means for removal in a practical setting. In general, O_3 is a strong electrophile and reacts quickly with alkenes and phenols, and more slowly or not at all with alkanes, aromatics with electron withdrawing substituents, and chlorinated solvents (Hoigne and Bader, 1983, I).

Table 1: Reaction Rate Constants with Molecular Ozone

Compound, M_i	$k_{M,O3}$, $M^{-1}s^{-1}$	Reference
Phenol	$1.3x10^3$	Hoigne and Bader, 1983, I
Benzene	2	Hoigne and Bader, 1983, I
Chlorobenzene	0.75	Hoigne and Bader, 1983, I
Trichloroethylene	15	Yao and Hoigne, 1991
Tetrachloroethylene	<0.1	Hoigne and Bader, 1983, I
Carbon Tetrachloride	<0.005	Hoigne and Bader, 1983, I

Hydroxyl Radical

$HO^{\cdot}$ is a powerful oxidant. The standard oxidation potential of $HO^{\cdot}$ is 2.80 volts, making it a stronger oxidant than O_3. Additionally, the reactions of compounds with $HO^{\cdot}$ are generally faster than the reactions with O_3. Rate constants for several compounds with $HO^{\cdot}$ are included in Table 2. $HO^{\cdot}$ will oxidize contaminants beginning with one of three types of reactions: radical addition, hydrogen abstraction, or electron transfer (Hoigne, 1982). The secondary radicals produced by these reactions can react with each other or with oxygen to form peroxy radicals, which may also act as strong oxidants (Hoigne, 1982).

Table 2: Reaction Rate Constants with the Hydroxyl Radical

Compound, M_i	$k_{M,OH}$, $M^{-1}s^{-1}$	Reference
Phenol	1.4×10^{10}	Field et al., 1982
Benzene	7.8×10^{9}	Buxton and Greenstock, 1988
Chlorobenzene	4.3×10^{9}	Kochany and Bolton, 1992
Trichloroethylene	2.9×10^{9}	Getoff, 1991
Tetrachloroethylene	2.3×10^{9}	Getoff, 1991
Carbon Tetrachloride	No Reaction	

The HO· radical is a relatively unselective oxidant and may react with a number of species other than the target compound. For modeling purposes, these species are regarded as scavengers, and play a major role in determining the effectiveness of AOP applications. The scavengers of primary interest for this project are the carbonate and bicarbonate ions, which have rate constants with HO· of 3.9×10^{8} $M^{-1}s^{-1}$ and 8.5×10^{6} $M^{-1}s^{-1}$ (Buxton and Greenstock, 1988) respectively. Other compounds, including natural organic matter (NOM), may also scavenge the radical (Staehelin and Hoigne, 1985), decreasing the efficiency of contaminant degradation.

2.2 Existing Models

2.2.1 O_3 and Micropollutant Models

Staehelin and Hoigne (1985) derived a kinetic model for the decomposition of O_3 with organic solutes acting as promoters and inhibitors of radical chain reactions. The chemical mechanism is shown in Figure 2 and includes the reactions shown in Figure 1, as well as reactions of O_3 and HO· with other natural water constituents. The reaction of a

micropollutant, M_i, occurs by two pathways: direct reaction with aqueous O_3 or reaction with $HO^{\cdot}$ radicals.

In natural waters, Staehelin and Hoigne postulated the presence of two types of natural organic substances that also react with O_3: direct reactors, D, that react with O_3 but do not produce radicals or radical-forming by-products, and promoters, P, which react with O_3 to form superoxide, $O_2^{\cdot-}$, or some other byproduct which propagates the radical chain.

The initiation for the radical chain reaction begins with the reaction between the OH^- and O_3 (From Figure 2, Reaction 4) or direct reaction of O_3 in an electron transfer reaction with other (unspecified) initiators, I (Reaction 3). Propagation of radical formation occurs via the reaction of superoxide ($O_2^{\cdot-}$) with O_3 to form the ozonide radical ($^{\cdot}O_3^-$) (Reaction 6). This then protonates to form HO_3 (Reaction 7) which decomposes to form $HO^{\cdot}$ (Reaction 8). Termination to the radical chain occurs when $HO^{\cdot}$ reacts with a scavenger such as a target micropollutant, M_i (Reaction 10). Other important scavengers, S_i (Reaction 11), include bicarbonate ions, carbonate ions and natural organic matter.

Figure 2: Reactions of Ozone in Natural Water

Initiation

1. $O_3 + M \rightarrow products$	$k_{M,O3}$ $M^{-1}s^{-1}$	
2. $O_3 + D \rightarrow products$	k_D	
3. $O_3 + I \rightarrow HO^\bullet + products$	k_I	
4. $OH^- + O_3 \rightarrow O_2^- + HO_2$	$k_{O_3,OH^-} = 70\ M^{-1}s^{-1}$	Staehelin and Hoigne, 1982
5. $HO_2 \leftrightarrow O_2^- + H^+$	$pK_a = 4.8$	

Propagation

6. $O_2^- + O_3 \rightarrow O_3^- + O_2$	$k_{O_2^-,O_3} = 1.6 \times 10^9\ M^{-1}s^{-1}$	Buhler et al., 1984
7. $O_3^- + H^+ \rightarrow HO_3$	$k_{O_3^-,H^+} = 5.2 \times 10^{10}\ M^{-1}s^{-1}$	Buhler et al., 1984
8. $HO_3 \rightarrow HO^\bullet + O_2$	$k_{HO_3} = 1.1 \times 10^5\ s^{-1}$	Buhler et al., 1984
9. $HO^\bullet + P \rightarrow products$	k_P	

Scavenging

10. $HO^\bullet + M \rightarrow products$	$k_{M,HO}$	
11. $HO^\bullet + S_i \rightarrow products$	$k_i S_i$	
12. $HO^\bullet + O_3 \rightarrow HO_2 + O_2$	$k_{OH,O_3} = 1.1 \times 10^8\ M^{-1}s^{-1}$	Buhler et al., 1984

I = Initiators, react with O_3 and form $HO^\cdot$.
D = Direct reactors, substances other than M which react with O_3 and do not produce radicals
P = Promoters, react with $HO^\cdot$ and form $O_2^\cdot$ which contributes to radical chain
S = Scavengers, substances other than M which react with $HO^\cdot$ and terminate radical reactions
M = Micropollutant

Based on this mechanism, the authors expressed O_3 depletion as shown below, assuming a steady state HO^- concentration.

$$-\left(\frac{d[O_3]}{dt}\frac{1}{[O_3]}\right) = k_{O_3,OH^-}[OH^-] + \{2k_{O_3,OH^-}[OH^-] + \sum k_{I,i}[M_i]\}\left(1 + \frac{\sum(k_{p,i}[M_i])}{\sum(k_{s,i}[M_i])}\right) = k_c' \qquad (4)$$

In this case, the scavenging term represents both scavenging by a micropollutant as well as scavenging by other compounds in the wastestream. As shown, the rate of O_3 depletion is first order in O_3 concentration even if the entire chain reaction is considered. Thus, it can be characterized by a pseudo-first-order rate constant, k_c'.

Yurteri (1988) developed the following empirical equation to describe O_3 decomposition as a function of pH, TOC, and alkalinity through correlating the O_3 decomposition rates of 96 synthetic water samples.

$$\log\frac{[O_3]}{[O_3]_o} = -3.98 + 0.66\,pH + 0.61\log(TOC) - 0.42\log\left(\frac{Alkalinity}{10}\right) \qquad (5)$$

$$\left(R^2 = 0.83\right)$$

This expression was also used to predict the O_3 decomposition rates of natural water samples with synthetic organic pollutants present.

Yurteri also derived a model to rationalize Equation 5 in terms of the Staehelin and Hoigne model. The Yurteri model assumed idealized plug flow in both liquid and gas flow. Additionally, it was assumed that the overall mass transfer coefficient, k_La, and the liquid phase holdup, h_L, were constant along the reactor column and that no gas phase reactions occurred. The model for organic compound removal consisted of four

equations: one each for O_3 and organic compound (M_i) in the liquid phase, and the same for the gas phase. These equations are shown below.

$$\frac{Q_L}{A}\frac{d[O_3]}{dz} = (K_L a)_{O_3}\left\{\frac{(O_3)}{H_{O_3}} - [O_3]\right\} - h_L w[O_3] \tag{6a}$$

$$\frac{Q_G}{A}\frac{d[O_3]}{dz} = (K_L a)_{O_3}\left\{\frac{(O_3)}{H_{O_3}} - [O_3]\right\} \tag{6b}$$

$$\frac{Q_L}{A}\frac{d[M]}{dz} = (K_L a)_{M}\left\{\frac{[M]}{H_{O_3}} - [M]\right\} - h_L k_T [M][O_3] \tag{6c}$$

$$\frac{Q_G}{A}\frac{d[M]}{dz} = (K_L a)_{M}\left\{\frac{[M]}{H_{O_3}} - [M]\right\} \tag{6d}$$

The term k_T in Equation 6c is the sum of the rate constants for O_3 decomposition (Equation 7) and depends on the scavenging capacity of a water, termed Ψ, which is the ratio of $HO^{\cdot}$ formation terms to $HO^{\cdot}$ scavenging terms (Equation 8).

$$k_T = k_D + k_I + \Psi(k_S + k_P) \tag{7}$$

$$\Psi = \frac{2k_{O_3,OH^-}[OH^-] + k_I[I]}{\sum k_i S_i} \tag{8}$$

Kelly (1991) developed a bi-phasic model for the prediction of O_3 decomposition as well as micropollutant (specifically PCE) decomposition. The decomposition rates of PCE and O_3 were divided into two regions, as shown in other work and experimental data

(Brodard et al., 1987). The two regions could be described as a fast O_3 decomposition region, followed by a slower decomposition region. It appeared that $HO^{\cdot}$ formation was highly efficient in region I, but in region II approached values comparable to those observed by Hoigne (1978) and others (Buxton et. al., 1988 and Peyton et. al., 1989).

2.2.2 O_3/H_2O_2 and Micropollutant Models

Glaze and Kang (1989a) developed a model to predict the oxidation of a micropollutant in the O_3/H_2O_2 system in a semi-batch reactor (batch liquid phase and a continuous flow gas phase). The principal reactions are shown in Figure 3.

Assuming a semi-batch reactor where O_3 enters at a partial pressure P (atm), the rate of destruction of an organic substrate was represented by the following.

$$-\frac{d\ln[M]}{dt} = k_{0,M} = k_S + k_{M,HO^{\cdot}}[HO^{\cdot}]_{SS} + k_{M,O_3}[O_3] \qquad (9)$$

k_s = sparging term
$k_{M,O3}$ = second order rate constant for O_3/ M_i reaction
$k_{M,HO^{\cdot}}$ = second order rate constant for $HO^{\cdot}$ / M_i reaction

For the Glaze and Kang model applied to PCE, it was assumed that sparging effects and direct reaction of M_i with O_3 were negligible when compared to oxidation by $HO^{\cdot}$.

Figure 3: Principal Reactions in the Glaze and Kang Model

Initiation

1. $H_2O_2 \leftrightarrow HO_2^- + H^+$	pK = 11.8	Behar et al., 1970
2. $HO_2^- + O_3 \rightarrow O_3^- + HO_2$	$k_{O_3,HO_2^-} = 5.5\text{x}10^6\ M^{-1}s^{-1}$	Staehelin and Hoigne, 1982
3. $OH^- + O_3 \rightarrow O_2^- + HO_2$	$k_{O_3,OH^-} = 70\ M^{-1}s^{-1}$	Staehelin and Hoigne, 1982
4. $HO_2 \leftrightarrow O_2^- + H^+$	$pK_a = 4.8$	Staehelin and Hoigne, 1982

Propagation

5. $O_2^- + O_3 \rightarrow O_3^- + O_2$	$k_{O_2^-,O_3} = 1.6\text{x}10^9\ M^{-1}s^{-1}$	Buhler et al., 1984
6. $O_3^- + H^+ \rightarrow HO_3$	$k_{O_3^-,H^+} = 5.2\text{x}10^{10}\ M^{-1}s^{-1}$	Buhler et al., 1984
7. $HO_3 \rightarrow HO^\bullet + O_2$	$k_{HO_3} = 1.1\text{x}10^5\ s^{-1}$	Buhler et al., 1984

Net equations for $HO^\bullet$ formation

8a. OH^- initiation	$3O_3 + OH^- \rightarrow 2HO^\bullet + 4O_2$
8b. HO_2^- initiation	$2O_3 + H_2O_2 \rightarrow 2HO^\bullet + 3O_2$

Radical Scavenging

9. $HO^\bullet + PCE \rightarrow products$	$k_{TCE,OH} = 2.9\text{x}10^9\ M^{-1}s^{-1}$	Getoff, 1991
10. $HO^\bullet + HO_2^- \rightarrow OH^- + HO_2$	$k_{OH,HO_2^-} = 7.5\text{x}10^9\ M^{-1}s^{-1}$	Christensen et al., 1982
11. $HO^\bullet + H_2O_2 \rightarrow H_2O + HO_2$	$k_{OH,H_2O_2} = 2.7\text{x}10^7\ M^{-1}s^{-1}$	Christensen et al., 1982
12. $HO^\bullet + S_i \rightarrow products$	k_iS_i	
13. $HO^\bullet + HCO_3^- \rightarrow H_2O + CO_3^-$	$k_{HCO_3^-,OH} = 8.5\text{x}10^6\ M^{-1}s^{-1}$	Buxton and Greenstock, 1988
14. $HO^\bullet + CO_3^{2-} \rightarrow OH^- + CO_3^-$	$k_{CO_3^{2-},OH} = 3.9\text{x}10^8\ M^{-1}s^{-1}$	Buxton and Greenstock, 1988
15. $HO^\bullet + O_3 \rightarrow HO_2 + O_2$	$k_{OH,O_3} = 1.1\text{x}10^8\ M^{-1}s^{-1}$	Buhler et al., 1984
16. $CO_3^- + H_2O_2 \rightarrow HO_2 + HCO_3^-$	$k_{H_2O_2,CO_3^-} = 8.0\text{x}10^5\ M^{-1}s^{-1}$	Behar et al., 1970
17. $CO_3^- + I_j \rightarrow CO_3^{2-} + I_j^-$		

To derive the steady state concentration for $HO^{\cdot}$, $[HO^{\cdot}]_{SS}$, it was assumed that the matrix was nearly pure water and that a large concentration of $HO^{\cdot}$ scavenger (other than O_3) was present. Additionally, $O_2^{\cdot-}$, $O_3^{\cdot-}$, $HO_3^{\cdot}$, and $HO^{\cdot}$ were assumed to be at steady state. The resulting expression for $[HO^{\cdot}]_{SS}$ is shown below.

$$[HO^{\bullet}]_{SS} = \frac{2k_2(10^{pH-pK})[H_2O_2][O_3]}{k_{M,HO^{\bullet}}[M] + \sum k_i S_i} \tag{10}$$

Substituting into Equation 14 and applying the assumption $k_{M,HO^{\cdot}} >> k_{M,O3}[O_3] + k_s$, the disappearance of micropollutant M_i was re-expressed as shown below.

$$-\frac{d\ln[M]}{dt} = k_{0,M} = k_{M,HO^{\bullet}}\left[\frac{2k_2(10^{pH-pK})[H_2O_2][O_3]}{k_{M,HO^{\bullet}}[M] + \sum k_i S_i}\right] \tag{11}$$

Using this equation as the basis for a kinetic model, Glaze and Kang found tests of the model demonstrated good agreement in mass transfer limited region of H_2O_2/O_3 ratios. For ratios below the stoichiometric optimum, results were less accurate. Experimental work verified that the model accurately predicted bicarbonate effects (Glaze and Kang, 1989b). Additionally, it was found that the O_3/H_2O_2 model could be used to evaluate the combined effect of scavengers in ground water.

Laplanche et al. (1995) have recently developed a semi-empirical model for ozonation bubble tower with or without hydrogen peroxide. The reactor volume was

divided into three zones and each zone was modeled as a series of continuous stirred tank reactors (CSTRs). A semi-empirical formula was used in concert with mass balance equations to predict the hydroxyl radical concentration. An additional semi-empirical equation described the O_3 consumption in the reactor.

The reactor was modeled as three separate zones which are characterized by different mixing conditions: the air arrival zone, the water arrival zone and the intermediate zone. The air arrival zone was modeled as one CSTR. In the water arrival zone mixing was significant. Finally, the intermediate zone was characterized by axial dispersion. To model an entire reactor, different percentages of the tank volume were attributed to each zone which was then characterized as a number (J) of CSTRs in series. For a CSTR, 100% of the tank volume would be described as water arrival zone with J1=1, while for a plug flow reactor (PFR) 100% of the tank volume would be described as water arrival zone, with J1>50. Standard conditions for a specific pilot plant are given below (LeSauze et al., 1992).

Figure 4: Typical Reactor Conditions for Laplanche et al. model

R1 = 25%	J1 = 2	(water arrival zone)
R2 = 50%	J2 = 4	(intermediate zone)
R3 = 25%	J3 = 1	(air arrival zone)

The degradation of a micropollutant M_i is given by the following:

$$r_M = \frac{dM}{dt} = -(k_D[O_3][M] + k_{ID}[HO^\bullet][M]) \qquad (12)$$

where k_D is the second order rate constant for direct reaction of M_i with O_3 and k_{ID} is the second order rate constant for the indirect reaction of M_i with $HO^{\cdot}$. Assuming that the hydroxyl radical concentration is proportional to O_3 concentration ($[HO^{\cdot}] = k'[O_3]$), the micropollutant removal rate was rewritten as shown.

$$r_M = \frac{dM}{dt} = -(k_D + k_{ID}k')[O_3][M] = -k_G[O_3][M] \tag{13}$$

Further, it was assumed that within a small elemental volume, the O_3 concentration was constant.

$$r_M = \frac{dM}{dt} = -k_G[O_3][M] = -k_T[M] \tag{14}$$

Mass balance equations were derived for O_3, H_2O_2 and $HO^{\cdot}$. The equation for O_3 consumption used a kinetic model. For the case of O_3 alone (no H_2O_2 addition), the equation was defined as follows:

$$Q_L[O_3]_i + \sum_0^{\Delta V} k_L a([O_3]^* - [O_3]_i) = Q_L[O_3]_R + \Delta V[O_3]_R\{k_D[M]_R + k_2[H_2O_2]_R 10^{pH-11.6} + w\} \tag{15}$$

where

Q_L = liquid phase flow rate

k_La = mass transfer coefficient

$[O_3]^*$ = liquid interface ozone concentration

ΔV = volume of the CSTR basic unit

$$\log w = -3.93 + 0.24\,pH + 0.7537\log(UVabsorbance\,@254nm) + 1.08\log(TOC) - 0.19\log(alkalinity)$$

For the O_3/H_2O_2 system, the w term in Equation 15, which accounts for the reaction of O_3 with HO^-, was replaced with k[HO^-] as defined below.

$$k_{HO\bullet,O_3}[HO^\bullet] = k_{HO\bullet,O_3}\frac{[O_3]\{2k_{O_3,OH^-}10^{pH-14} + 2k_{O_3,HO_2^-}10^{pH-11.6}[H_2O_2] + \sum k_{Ii}[I]\}}{k_{ID}[M] + [HCO_3^-]\left(k_{HCO_3^-,HO\bullet} + k_{CO_3^{-2},HO\bullet}10^{pH-10.25}\right)\sum k_{Si}[S]} \qquad (16)$$

The mass balance on H_2O_2 is given in Equation 17.

$$Q_L[H_2O_2]_e = Q_L[H_2O_2] + \Delta V[H_2O_2]\{k_{O_3,HO_2^-}10^{pH-11.6}[O_3] + (k_{H_2O_2,HO}10^{pH-11.6} + k_{HO_2^-,HO})[HO^\bullet]\} \qquad (17)$$

Finally, the mass balance on HO^- was described as shown below.

$$[HO^\bullet] = k'[O_3] = \left[\frac{[O_3]\{2k_{O_3,OH^-}10^{pH-14} + 3.16\times10^{-7}*10^{0.42pH}TOC + 2k_{O_3,HO_2^-}10^{pH-11.6}[H_2O_2]\}}{k_{ID}[M] + [HCO_3^-](k_{HCO_3^-,HO\bullet} + k_{CO_3^{-2},HO\bullet}10^{pH-10.25})}\right] \qquad (18)$$

In summary, the Laplanche et al. model can be summarized as a semi-empirical model which incorporates a combination of mechanistic equations and empirical correlations. The steady state model results compared well to data from three papers. Additionally, researchers anticipated that the model would, in the future, be capable of predicting the evolution of the first oxidation metabolites.

3. FORMULATION

3.1 Chemistry

The mechanism for the oxidation of a micro-pollutant in the O_3/H_2O_2 system is shown in Figure 5. As shown in Reactions 8 and 9, contaminant removal in the O_3/H_2O_2 system may occur via two pathways: direct oxidation by molecular O_3 or oxidation by $HO^{\cdot}$ (Hoigne and Bader, 1975). The mechanism shown is essentially the Glaze and Kang mechanism, previously shown in Figure 3, with several modifications.

For completeness, several reactions are included in the current mechanism which were not in the published Glaze and Kang mechanism. The current mechanism includes both micropollutant removal pathways, despite the slow rate constant for direct oxidation by O_3. The carbonate radical reaction with the conjugate base of hydrogen peroxide was included. Additionally, several radical-radical recombination reactions are included in Reactions 17 through 19. Reactions 17 and 18 are the recombination of the hydroperoxyl radical with itself and with its conjugate base, superoxide. The recombination of carbonate radicals is included in Reaction 19. Note that the mechanism still includes several reactions which form unknown products, particularly Reactions 8, 9, and 19.

Equilibria equations describing the deprotonation of several species have also been included. The equilibrium constraints manifest themselves as a system of algebraic equations which must be applied to the system of partial differential equations (PDEs) derived from the reaction mechanism discussed above. Each of these equilibria equations must be satisfied spatially and temporally for any correct solution of the system of equations. The equilibria, which are shown in Figure 6, include those for carbonate

species, hydrogen peroxide, superoxide radical as well as pH, which acts as the master variable for a system in which speciation is important.

With the mechanism thus described, the appropriate transport equation is used to develop the appropriate set of equations to describe the O_3/H_2O_2 destruction of a micropollutant.

Figure 5: Mechanism for Ozone/Peroxide Oxidation of TCE

Initiation

1. $H_2O_2 \leftrightarrow HO_2^- + H^+$	pK = 11.8	Behar et al., 1970
2. $HO_2^- + O_3 \rightarrow O_3^- + HO_2$	$k_{O_3,HO_2^-} = 5.5\text{x}10^6\ M^{-1}s^{-1}$	Staehelin and Hoigne, 1982
3. $OH^- + O_3 \rightarrow O_2^- + HO_2$	$k_{O_3,OH^-} = 70\ M^{-1}s^{-1}$	Staehelin and Hoigne, 1982
4. $HO_2 \leftrightarrow O_2^- + H^+$	pK = 4.8	Staehelin and Hoigne, 1982

Propagation

5. $O_2^- + O_3 \rightarrow O_3^- + O_2$	$k_{O_2^-,O_3} = 1.6\text{x}10^9\ M^{-1}s^{-1}$	Buhler et al., 1984
6. $O_3^- + H^+ \rightarrow HO_3$	$k_{O_3^-,H^+} = 5.2\text{x}10^{10}\ M^{-1}s^{-1}$	Buhler et al., 1984
7. $HO_3 \rightarrow OH + O_2$	$k_{HO_3} = 1.1\text{x}10^5\ s^{-1}$	Buhler et al., 1984

Destruction and Scavenging

8. $TCE + O_3 \rightarrow products$	$k_{TCE,O_3} = 15\ M^{-1}s^{-1}$	Yao and Hoigne, 1991
9. $OH + TCE \rightarrow products$	$k_{TCE,OH} = 2.9\text{x}10^9\ M^{-1}s^{-1}$	Getoff, 1991
10. $OH + HO_2^- \rightarrow OH^- + HO_2$	$k_{OH,HO_2^-} = 7.5\text{x}10^9\ M^{-1}s^{-1}$	Christensen et al., 1982
11. $OH + H_2O_2 \rightarrow H_2O + HO_2$	$k_{OH,H_2O_2} = 2.7\text{x}10^7\ M^{-1}s^{-1}$	Christensen et al., 1982
12. $OH + HCO_3^- \rightarrow H_2O + CO_3^-$	$k_{HCO_3^-,OH} = 8.5\text{x}10^6\ M^{-1}s^{-1}$	Buxton and Greenstock, 1988
13. $OH + CO_3^{2-} \rightarrow OH^- + CO_3^-$	$k_{CO_3^{2-},OH} = 3.9\text{x}10^8\ M^{-1}s^{-1}$	Buxton and Greenstock, 1988
14. $OH + O_3 \rightarrow HO_2 + O_2$	$k_{OH,O_3} = 1.1\text{x}10^8\ M^{-1}s^{-1}$	Buhler et al., 1984
15. $CO_3^- + H_2O_2 \rightarrow HO_2 + HCO_3^-$	$k_{H_2O_2,CO_3^-} = 8.0\text{x}10^5\ M^{-1}s^{-1}$	Behar et al., 1970
16. $CO_3^- + HO_2^- \rightarrow O_2^- + HCO_3^-$	$k_{HO_2^-,CO_3^-} = 5.6\text{x}10^7\ M^{-1}s^{-1}$	Behar et al., 1970
17. $HO_2 + HO_2 \rightarrow O_2 + H_2O_2$	$k_{HO_2,HO_2} = 8.3\text{x}10^5\ M^{-1}s^{-1}$	Bielski et al., 1985
18. $O_2^- + HO_2 + H_2O \rightarrow O_2 + H_2O_2 + OH^-$	$k_{HO_2,O_2^-} = 9.7\text{x}10^7\ M^{-1}s^{-1}$	Bielski et al., 1985
19. $CO_3^- + CO_3^- \rightarrow products$	$k_{CO_3^-} = 2.2\text{x}10^6\ M^{-1}s^{-1}$	Huie and Clefton, 1990

Figure 6: Equilibrium Constants for O_3/H_2O_2 System

1. Hydrogen Peroxide	$K_a = \frac{[H^+][HO_2^-]}{[H_2O_2]} = 10^{-11.8}$	(Behar et al., 1970)
2. Superoxide	$K_a = \frac{[H^+][O_2^-]}{[HO_2]} = 10^{-4.8}$	(Staehelin and Hoigne, 1982)
3. Bicarbonate	$K_a = \frac{[H^+][HCO_3^-]}{[H_2CO_3^*]} = 10^{-6.3}$	(Snoeyink and Jenkins, 1980)
4. Carbonate	$K_a = \frac{[H^+][CO_3^{2-}]}{[HCO_3^-]} = 10^{-10.3}$	(Snoeyink and Jenkins, 1980)
5. Water	$K_w = [H^+][OH^-] = 10^{-14}$	(Stumm and Morgan, 1970)

3.2 *Transport*

The typical reactor used in the United States for O_3/H_2O_2 oxidation is a bubble contactor (Marinas et al., 1993). The fluid and gas phases can be flowing in the same direction (co-current) or in opposite directions (counter-current). In an ideal system of this type, both the gas and fluid phases are generally plug flow with limited dispersion, for which the appropriate transport equation is the Advective/Dispersive/Reactive (ADR) equation as shown in Equation 19. As shown for species *i* in phase α, the equation includes an accumulation term, as well as terms for dispersion, advection, reaction, mass transfer and an internal source/sink. For a co-current system, the influent and effluent boundary conditions and initial conditions are shown in Equations 20, 21 and 22, respectively. Slight modifications can accommodate counter current systems.

$$\frac{\partial C_{i,\alpha}}{\partial t} = D_\alpha \frac{\partial^2 C_{i,\alpha}}{\partial z^2} - \upsilon_\alpha \cdot \frac{\partial C_{i,\alpha}}{\partial z} + \left(\frac{\partial C_{i,\alpha}}{\partial t}\right)_{RXN} + \left(\frac{\partial C_{i,\alpha}}{\partial t}\right)_{MT} + \Gamma(C_{i,\alpha}) \qquad (19)$$

Where:
D_α = Dispersion Coefficient in phase α
$C_{i,\alpha}$ = Concentration of species *i* in phase α
v_α = Velocity of phase α
Γ_α = Source/sink term in phase α

$$\upsilon_\alpha C_{i,\alpha}^{inf} = \upsilon_\alpha C_{i,\alpha}^{0} - D_\alpha \frac{\partial C_{i,\alpha}^{0}}{\partial z} \qquad (20)$$

Where:

$C_{i,\alpha}^{inf}$ = Influent concentration of species *i* in phase α
$C_{i,\alpha}^{0}$ = Concentration at z = 0 of species *i* in phase α

$$\frac{\partial C_{i,\alpha}^{L}}{\partial z} = 0 \tag{21}$$

Where:

$C_{i,\alpha}^{L}$ = Concentration at z = L of species *i* in phase α

$$C_{i,\alpha} = C_{i,\alpha}^{init} \tag{22}$$

Where:

$C_{i,\alpha}^{init}$ = Initial concentration of species *i* in phase α

Dispersion and velocity terms will be phase dependent as indicated. Although the source/sink term is included in this ADR form, it can be neglected for this system because no internal sources and sinks exist. For the O_3/H_2O_2 system, the reaction term includes formation and disappearance terms for each species as derived from the mechanism in Figure 5. Each reaction must be included in the corresponding PDEs for each product and reactant involved in that reaction. Additionally, the reaction term includes a series of reversible reaction terms representing the equilibria identified in Figure 6. These liquid phase dissociation terms can be incorporated as forward and reverse reactions for each equilibrium constant.

Mass transfer between the gas and liquid phases must also be included, although it is not required for each species in the system. In particular, O_3 is transferred from the gas phase to the liquid phase in a bubble contactor and, if the contaminant is volatile, there may be sparging of the contaminant into the gas phase. It is also possible that there will be

mass transfer between the phases for both oxygen and carbon dioxide, the latter of which is in indirect equilibrium with the carbonate species $H_2CO_3^*$.

3.3 System of Equations

3.3.1 ADR equations for each species

With the correct transport equations selected, a system of partial differential equations can be derived to describe the changes in concentrations for each species in the O_3/H_2O_2 system. This is done by expanding each of the terms shown in the ADR equation in Equation 19. These expressions are shown in Figure 7. An ADR equation is written to describe each species in the system, as shown there are 19. Each equation includes formation and loss terms for the species as derived from the mechanism previously shown in Figure 5, as well as the appropriate fast, reversible reaction terms representing the equilibria constants shown in Figure 6.

The system of equations as shown in Figure 7 is a system of coupled, stiff, nonlinear PDEs. The equations are second order, due to the dispersion term, and are classified as parabolic. The complex chain reaction in the O_3/H_2O_2 mechanism determines the coupled nature of the PDEs, as most of the reactions are second order (nonlinear) overall and first order with respect to two different species. The variation in rate constants (see Figure 5) gives rise to widely varying time scales, which defines the system as stiff.

Figure 7: ADR Equations for Species in the Ozone/Peroxide System

Liquid Phase Ozone

$$\frac{\partial[O_3]}{\partial t} = D_l \frac{\partial^2[O_3]}{\partial z^2} - \upsilon_l \frac{\partial[O_3]}{\partial z} - k_{O_3,OH^-}[O_3][OH^-] - k_{O_3,HO_2^-}[HO_2^-][O_3] - k_{O_2^-,O_3}[O_2^-][O_3]$$
$$-k_{OH,O_3}[O_3][HO^\bullet] - k_{M,O_3}[M][O_3] + \frac{k_L a}{\theta_w}\left(\frac{[O_3]_g}{H_{O_3}} - [O_3]\right)$$

Gas Phase Ozone

$$\frac{\partial[O_3]_g}{\partial t} = D_g \frac{\partial^2[O_3]_g}{\partial z^2} - \upsilon_g \frac{\partial[O_3]_g}{\partial z} - \frac{k_L a}{\theta_w}\left(\frac{[O_3]_g}{H_{O_3}} - [O_3]\right)$$

Liquid Phase M_i

$$\frac{\partial[M]}{\partial t} = D_l \frac{\partial^2[M]}{\partial z^2} - \upsilon_l \frac{\partial[M]}{\partial z} - k_{M,HO^\bullet}[M][HO^\bullet] - k_{M,O_3}[O_3][M] + \frac{k_L a}{\theta_w}\left(\frac{[M]_g}{H_M} - [M]\right)$$

Gas Phase M_i

$$\frac{\partial[M]_g}{\partial t} = D_g \frac{\partial^2[M]_g}{\partial z^2} - \upsilon_g \frac{\partial[M]_g}{\partial z} - \frac{k_L a}{\theta_w}\left(\frac{[M]_g}{H_M} - [M]\right)$$

Hydrogen Peroxide

$$\frac{\partial[H_2O_2]}{\partial t} = D_l \frac{\partial^2[H_2O_2]}{\partial z^2} - \upsilon_l \frac{\partial[H_2O_2]}{\partial z} - k_{HO^\bullet,H_2O_2}[H_2O_2][HO^\bullet] - k_{H_2O_2,CO_3^-}[H_2O_2][CO_3^-] + k_{HO_2,HO_2}[HO_2]^2 + k_{HO_2,O_2^-}[HO_2][O_2^-]$$
$$-k^F_{H_2O_2,HO_2^-}[H_2O_2] + k^R_{H_2O_2,HO_2^-}[HO_2^-][H^+]$$

Figure 7: ADR Equations for Species in the Ozone/Peroxide System

Conjugate Base of Hydrogen Peroxide

$$\frac{\partial[HO_2^-]}{\partial t} = D_l \frac{\partial^2[HO_2^-]}{\partial z^2} - \upsilon_l \frac{\partial[HO_2^-]}{\partial z} - k_{HO^\bullet, H_2O^-}[HO_2^-][HO^\bullet] - k_{O_3, HO_2^-}[HO_2^-][O_3]_l - k_{HO_2^-, CO_3^-}[HO_2^-][CO_3^-] + k^F_{H_2O_2, HO_2^-}[H_2O_2] - k^R_{H_2O_2, HO_2^-}[HO_2^-][H^+]$$

Oxygen

$$\frac{\partial[O_2]}{\partial t} = D_l \frac{\partial^2[O_2]}{\partial z^2} - \upsilon_l \frac{\partial[O_2]}{\partial z} + k_{O_2^-, O_3}[O_2^-][O_3^-] + k_{HO_3}[HO_3] + k_{HO^\bullet, O_3}[HO^\bullet][O_3] + k_{HO_2, HO_2}[HO_2]^2 + k_{HO_2, O_2^-}[HO_2][O_2^-]$$

Carbonate

$$\frac{\partial[CO_3^{2-}]}{\partial t} = D_l \frac{\partial^2[CO_3^{2-}]}{\partial z^2} - \upsilon_l \frac{\partial[CO_3^{2-}]}{\partial z} - k_{CO_3^{2-}, HO^\bullet}[HO^\bullet][CO_3^{2-}] + k^F_{HCO_3^-, CO_3^{2-}}[HCO_3^-] - k^R_{HCO_3^-, CO_3^{2-}}[CO_3^{2-}][H^+]$$

Bicarbonate

$$\frac{\partial[HCO_3^-]}{\partial t} = D_l \frac{\partial^2[HCO_3^-]}{\partial z^2} - \upsilon_l \frac{\partial[HCO_3^-]}{\partial z} - k_{H_2O_2, CO_3^-}[H_2O_2][CO_3^-] - k_{HO_2^-, CO_3^-}[HO_2^-][CO_3^-] - k_{HCO_3^-, HO^\bullet}[HCO_3^-][HO^\bullet]$$
$$+ k^F_{H_2CO_3, HCO_3^-}[H_2CO_3] - k^R_{H_2CO_3, HCO_3^-}[HCO_3^-][H^+] - k^F_{HCO_3^-, CO_3^{2-}}[HCO_3^-] + k^R_{HCO_3^-, CO_3^{2-}}[CO_3^{2-}][H^+]$$

Carbonic Acid

$$\frac{\partial[H_2CO_3]}{\partial t} = D_l \frac{\partial^2[H_2CO_3]}{\partial z^2} - \upsilon_l \frac{\partial[H_2CO_3]}{\partial z} + \frac{k_L a}{\theta_w}\left(\frac{[CO_2]_g}{H_M} - [H_2CO_3]\right) - k^F_{H_2CO_3, HCO_3^-}[H_2CO_3] + k^R_{H_2CO_3, HCO_3^-}[HCO_3^-][H^+]$$

Carbon Dioxide

$$\frac{\partial[CO_2]_g}{\partial t} = D_g \frac{\partial^2[CO_2]_g}{\partial z^2} - \upsilon_g \frac{\partial[CO_2]_g}{\partial z} - \frac{k_L a}{\theta_w}\left(\frac{[CO_2]_g}{H_M} - [H_2CO_3]\right)$$

Figure 7: ADR Equations for Species in the Ozone/Peroxide System

Carbonate Radical

$$\frac{\partial[CO_3^-]}{\partial t} = D_l \frac{\partial^2[CO_3^-]}{\partial z^2} - v_l \frac{\partial[CO_3^-]}{\partial z} - k_{H_2O_2,CO_3^-}[H_2O_2][CO_3^-] - k_{HO_2^-,CO_3^-}[HO_2^-][CO_3^-] - k_{HO^\bullet,HCO_3^-}[HO^\bullet][HCO_3^-]$$
$$-k_{HO^\bullet,CO_3^{2-}}[HO^\bullet][CO_3^{2-}] - 2k_{CO_3^-,CO_3^-}[CO_3^-]^2$$

Ozonide Radical

$$\frac{\partial[O_3^-]}{\partial t} = D_l \frac{\partial^2[O_3^-]}{\partial z^2} - v_l \frac{\partial[O_3^-]}{\partial z} + k_{HO_2^-,O_3}[HO_2^-][O_3] + k_{O_2^-,O_3}[O_2^-][O_3] - k_{O_3^-,H^+}[O_3^-][H^+]$$

Super Oxide

$$\frac{\partial[O_2^-]}{\partial t} = D_l \frac{\partial^2[O_2^-]}{\partial z^2} - v_l \frac{\partial[O_2^-]}{\partial z} + k_{OH^-,O_3}[O_3]_l[OH^-]_l - k_{O_2^-,O_3}[O_2^-][O_3]_l - k_{HO_2^-,CO_3^-}[HO_2^-][CO_3^-] - k_{HO_2,O_2^-}[HO_2][O_2^-]$$
$$+k^F_{HO_2^-,O_2^-}[HO_2^-] - k^R_{HO_2^-,O_2^-}[O_2^-][H^+]$$

Peroxy-Radical

$$\frac{\partial[HO_2]}{\partial t} = D_l \frac{\partial^2[HO_2]}{\partial z^2} - v_l \frac{\partial[HO_2]}{\partial z} + k_{OH,H_2O_2}[H_2O_2][OH] + k_{HO^\bullet,HO_2^-}[HO_2^-][HO^\bullet] - k_{OH^-,O_3}[O_3][OH^-] + k_{OH^\bullet,O_3}[O_3][HO^\bullet]$$
$$k_{H_2O_2,CO_3^-}[H_2O_2][CO_3^-] - 2k_{HO_2,HO_2}[HO_2]^2 - k_{O_3,HO_2^-}[O_3][HO_2^-] - k^F_{HO_2^-,O_2^-}[HO_2^-] + k^R_{HO_2^-,O_2^-}[O_2^-][H^+]$$

HO_3

$$\frac{\partial[HO_3]}{\partial t} = D_l \frac{\partial^2[HO_3]}{\partial z^2} - v_l \frac{\partial[HO_3]}{\partial z} + k_{O_3^-,H^+}[O_3^-][H^+] - k_{HO_3}[HO_3]$$

Figure 7: ADR Equations for Species in the Ozone/Peroxide System

Liquid Phase Hydroxyl Radical

$$\frac{\partial[HO^\bullet]}{\partial t} = D_l \frac{\partial^2[HO^\bullet]}{\partial z^2} - \upsilon_l \frac{\partial[HO^\bullet]}{\partial z} + k_{HO_3}[HO_3] - k_{M,HO^\bullet}[HO^\bullet][M] - k_{HO^\bullet,H_2O_2}[H_2O_2][HO^\bullet] - k_{HO^\bullet,HO_2^-}[HO_2^-][HO^\bullet]$$
$$-k_{HCO_3^-,HO^\bullet}[HO^\bullet][HCO_3^-] - k_{CO_3^{2-},HO^\bullet}[HO^\bullet][CO_3^{2-}] - k_{HO^\bullet,O_3}[HO^\bullet][O_3]$$

Hydrogen Ion

$$\frac{\partial[H^+]}{\partial t} = D_l \frac{\partial^2[H^+]}{\partial z^2} - \upsilon_l \frac{\partial[H^+]}{\partial z} - k_{O_3^-,H^+}[O_3^-][H^+] + k^F_{HO_2^-,O_2^-}[HO_2^-] - k^R_{HO_2^-,O_2^-}[O_2^-][H^+] + k^F_{H_2CO_3,HCO_3^-}[H_2CO_3] - k^R_{H_2CO_3,HCO_3^-}[HCO_3^-][H^+]$$
$$+k^F_{HCO_3^-,CO_3^{2-}}[HCO_3^-] - k^R_{HCO_3^-,CO_3^{2-}}[CO_3^{2-}][H^+] + k^F_{H_2O_2,HO_2^-}[H_2O_2] - k^R_{H_2O_2,HO_2^-}[HO_2^-][H^+] + k^F_w[H_2O] - k^R_w[H^+][OH^-]$$

Hydroxide Ion

$$\frac{\partial[OH^-]}{\partial t} = D_l \frac{\partial^2[OH^-]}{\partial z^2} - \upsilon_l \frac{\partial[OH^-]}{\partial z} - k_{O_3^-,OH^-}[O_3^-][OH^-] + k_{CO_3^{2-},OH}[OH][CO_3^{2-}] + k_{HO_2,O_2^-}[HO_2][O_2^-] + k_{OH,HO_2^-}[HO_2^-][OH]_l$$
$$+k^F_w[H_2O] - k^R_w[H^+][OH^-]$$

3.3.2 Assumptions & Simplifications

The model of the O_3/H_2O_2 system consists of the numerical solution to the equations presented in the previous sections. Some assumptions and simplifications are necessary to promote the development of a model with practical computing and memory requirements. The model does allow for co-current or counter-current reactors as well as changes in influent concentrations with time, but constant (steady-state) flow rates for the gas and liquid phases are assumed. Additionally, changes in bubble size due to mass transfer, changing pressure, and aggregation are neglected.

3.4 Generalized Approach

Sections 3.1 through 3.3 describe the specific problem at hand. However, the approach to developing the actual model is a very general one, based on the type of mathematical problem that will arise from similar physical systems. Of particular importance for this approach is the development of a generalized input file.

3.4.1 Generalized Input File

To maximize the utility of the model, it is necessary to develop a generalized input file format. This prevents the hard wiring of the code specific to one type of AOP or one specific micropollutant. The file format must be user-friendly and allow for changes in the mechanism without requiring changes in the actual computer code of the model. The format used for this model (Pedit, 1995) is similar to that developed by Jeffries and co-workers (1993). This approach allows the user to give numerical information to describe the reaction mechanism, the equilibria constraints, initial and input conditions. The code

then reads the file and creates the appropriate system of discretized PDEs to solve. Any problem that fits into the specified file format can be solved using this code, which allows for maximum flexibility. It also saves the user from the tedious process of developing the system of equations to describe an individual problem, such as those shown in Figure 5.

An example of a complete input file is included in Appendix A. The first section of the input file contains parameters for the numerical method. These include absolute and relative tolerances for the solver, which describe the accuracy of the desired solution. The user may also specify the number of elements, the order of the basis functions used to integrate the equations, and the number of Gauss points for each element.

Reactor information is contained in the next section of the input file. This includes dimensions of the reactor, flow rates for both liquid and gas phases, volume fractions for solid, liquid and gas phases, as well as the dispersion coefficients for liquid and gas phases. The program calculates the phase velocities from the provided input.

The next section of the input file describes the species in the system of PDEs. Each species is named and then assigned a number as it is read by the program. The water phase and gas phase indicators can be set for the species to exist in either or both phases. If the species exists in both phases, then a Henry's constant and a mass transfer coefficient are specified to describe mass transfer between the phases.

The reaction mechanism is then input into the data file. Each reaction is assigned a number as it is read by the program and can be assigned to the liquid or gas phase. Up to three reactants are listed, as well as up to three products, followed by the stoichiometry for each species involved in the reaction.

Equilibria data are also incorporated into the data file. Each constraint is assigned a number as it is read by the program. Then, similarly to the reaction input, up to three products and reactants and their respective stoichiometries are specified. This completes the data required to run the program.

3.5 Numerical Solution

With the system of equations described, a numerical method for solving the system can be selected. As described in section 3.3.1 the equations in Figure 5 are coupled, stiff, nonlinear partial differential equations. Each of these qualities is important to consider when selecting a numerical methods approach.

3.5.1 Method of Lines

A common approach to solving engineering systems of PDEs is to use the Method of Lines (MOL). MOL transforms the system of PDEs into a system of ODEs, generally by discretizing the domain using either finite element or finite difference methods (FEM or FDM). This reduces the system of PDEs to a system of temporal ODEs, which can then be solved using one of the many ODE solvers that are currently available. Brenan et al. (1989) identify two major advantages to using MOL. First, the approach is computationally efficient, allowing the ODE solvers, which are generally coded to be robust and efficient, to discretize time and choose appropriate time steps. Additionally, in using MOL, one need only be concerned with setting the increment for spatial derivatives, allowing the solver to handle temporal increments, which simplifies the coding significantly.

3.5.2 Solver Required for Solution

Several factors influence the selection of a solver for a problem of this type. As was mentioned previously, the equations describing this system are stiff, coupled PDEs. Once reduced by MOL, the system is a large system of ODEs, requiring the use of an ODE solver which can handle stiff systems of equations. Generally, stiff systems are handled using implicit methods, with the backward difference formula (BDF) a common choice (Miller, 1995).

The DAE solver DDASSL (Petzold, 1983) was selected as the solver for this model. DDASSL is specifically designed to handle differential algebraic equations or ODEs, and relies on BDF, making it a good candidate for stiff systems of ODEs. Specifically, DDASSL is designed to handle systems of the form:

$$F(t, y(t), y'(t)) = 0 \tag{23a}$$

$$y(t_0) = y_0 \tag{23b}$$

$$y'(t_0) = y_0' \tag{23c}$$

DDASSL requires a subroutine called RES, which is a user written routine describing the function F as shown in Equations 23a, 23b, and 23c. Given an input time T, and vectors of Y and YPRIME, RES produces an output vector DELTA, which is a measure of how far F is from being equal to zero. DDASSL has several other options, which are covered in the program prologue (Petzold, 1983).

4. RESULTS AND DISCUSSION

The model developed based on the previous discussions was written by Dr. Joseph A. Pedit. Preliminary model verification performed using analytical solutions for simplified cases of the ADR equation (Parker and van Genuchten, 1984) showed good agreement with model predictions. The sensitivity of the model to varying conditions was investigated and a preliminary comparison to real contactor data was conducted. Results and discussion of both series of tests follow.

4.1 Sensitivity

The Los Angeles Department of Water and Power (LADWP) has constructed a plant with two co-current, packed bed O_3/H_2O_2 contactors to treat groundwater contaminated with PCE and TCE. Operating conditions from several performance tests were obtained from LADWP personnel (Karimi, 1995) to assist in the development of a realistic input file for the model. The baseline influent concentrations and input parameters derived from the LADWP data are summarized in Table 3. A brief description of the selected values for k_La, D_L, and D_G is provided in Section 4.2. The data were used to run several series of model runs to investigate the response of the model to varying conditions. Following are discussions of the model results for transient response of the O_3/H_2O_2 system at start-up, varying the rate constant of M_i with $HO^{\cdot}$, varying mass transfer coefficient, varying dispersion in both liquid and gas phases, varying carbonate levels, varying influent pH, reactor configuration and preliminary comparison with concentration profile data from LADWP. Trials were run to 1000 seconds to reach steady state. Results are shown as steady state concentration profiles versus the dimensionless length

(the location of the concentration in the reactor divided by the total reactor length). Except as noted, the gas and liquid phases were co-current.

Table 3: Data file - Baseline Conditions

Parameter	Value	Units
Gas Flow Rate	0.028	m^3/s
Liquid Flow Rate	0.135	m^3/s
Tank Depth	3.8	m
Tank Cross Section	6.925	m^2
D_L	0.04	m^2/s
D_G	0.4	m^2/s
k_La	0.005	s^{-1}
Influent $[O_3]_l$	0.00	M
Influent $[H_2O_2]_l$	7.06×10^{-5}	M
Influent pH	7.8	-
Influent $[IC]_T$	1.00×10^{-3}	M
Influent $[TCE]_l$	7.64×10^{-6}	M
Influent $[O_3]_g$	3.5×10^{-4}	M

4.1.1 Transient Model Predictions

The transient response trials assume that the influent stream had reached steady state in the reactor, then at time equal zero, both H_2O_2 and O_3 were turned on. The concentration profiles for both TCE and $HO^{\cdot}$ are shown in Figures 8 and 9, respectively.

Figure 8 shows that within 25 seconds after H_2O_2 and O_3 start-up, the model predicts a TCE concentration drop of 10 %. Under these conditions, the steady state concentration profile is reached after approximately 300 seconds, about 2.5 bed-volumes for the assumed reactor. TCE degradation is greatest in the first half of the reactor, where

concentrations are high enough to compete with CO_3^{2-} for $HO^{\cdot}$. At the influent of the reactor ($L/L_o = 0$), the concentration of TCE drops due to dispersion, as represented in the influent boundary condition previously shown in Equation 20. As the reaction proceeds and the TCE concentration drops throughout the reactor, the initial dispersion drop increases as is expected.

Initial $HO^{\cdot}$ concentration is zero in the reactor. Figure 9 shows that within 50 seconds, the model predicts a concentration profile in the reactor on the order of 10^{-12} M. The steady state profile shows a low concentration near the influent of the reactor, consistent with the high removal of TCE in the same vicinity. As the concentration of TCE drops, the $HO^{\cdot}$ concentration increases to over $3x10^{-11}$ M.

Figure 8: Approach to Steady State Concentration Profile for TCE under baseline conditions

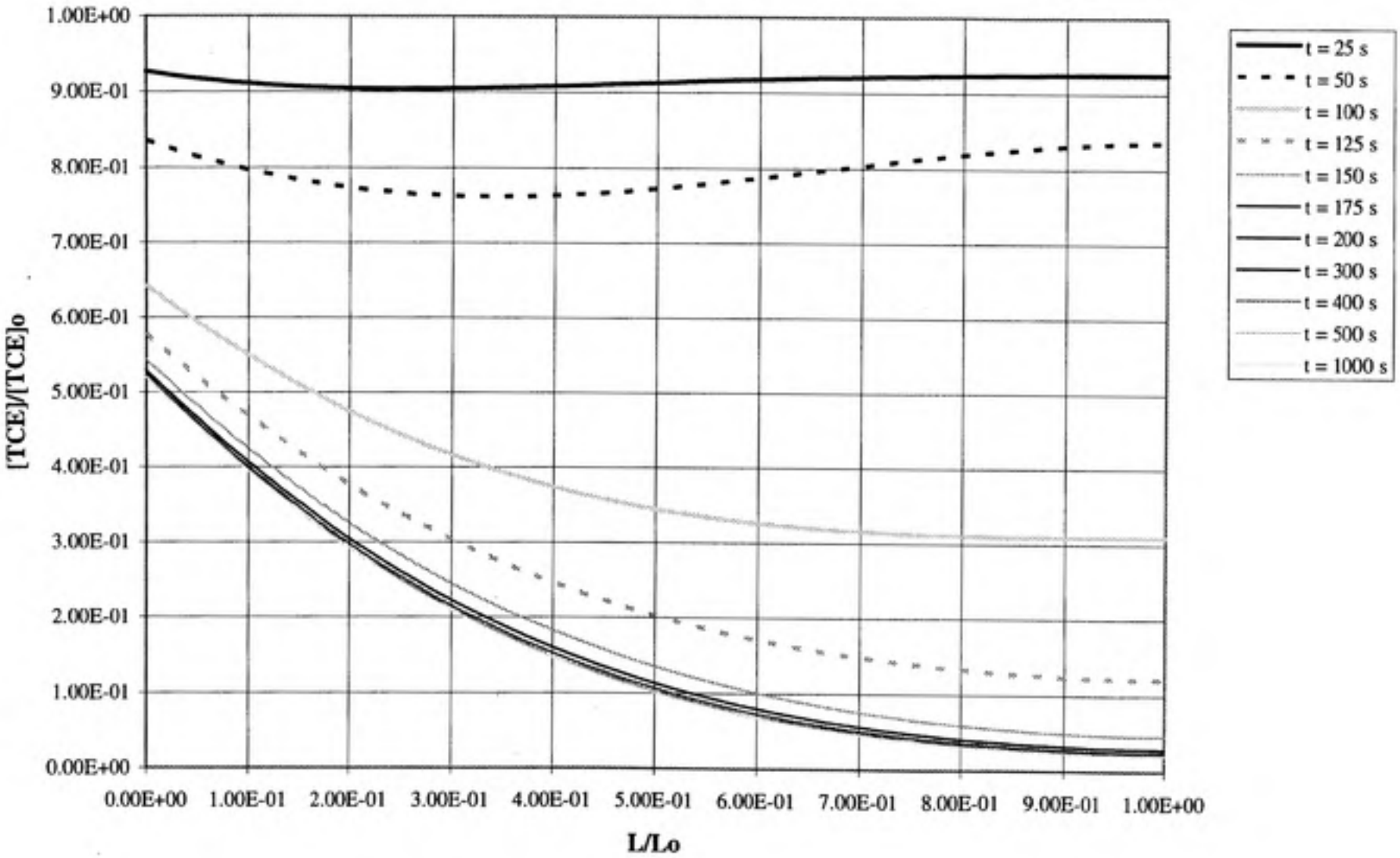

Figure 9: Approach to Steady State Concentration Profile for HO under baseline conditions

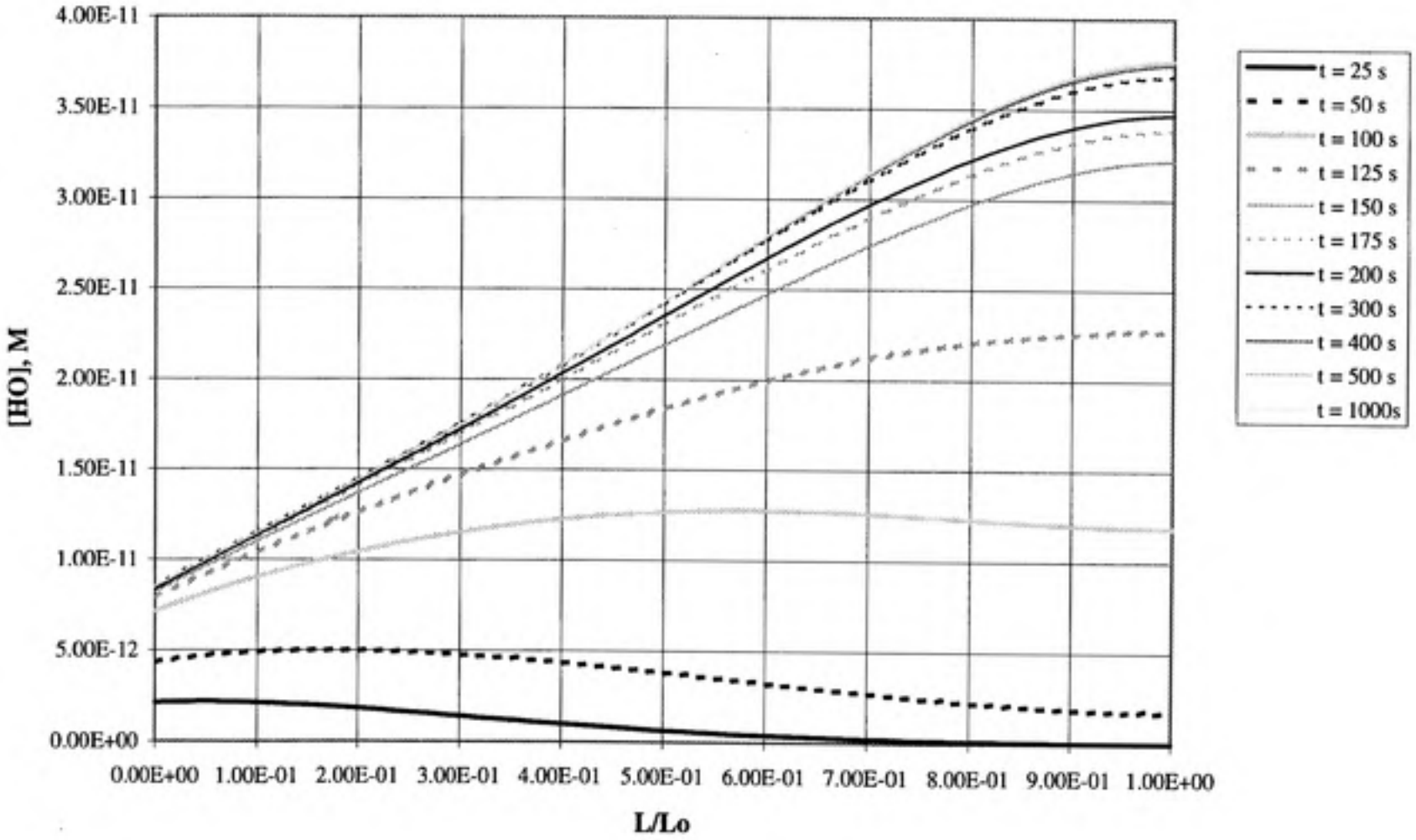

4.1.2 Rate Constant of Micropollutant with HO·

Trials were run using baseline conditions and varying the rate constants of some micropollutant, M_i, with HO· ($k_{M,HO}$) from $1x10^1$ to $1x10^{10}$ $M^{-1}s^{-1}$. The results of these trials are shown in Figure 10 as steady state concentration profiles.

For the specified concentrations, the model predicts that compounds with rate constants below $1x10^6$ $M^{-1}s^{-1}$ are not competitive with the reaction between HO· and the bicarbonate and carbonate ions and micropollutant destruction is low. The model predicts a slight improvement for rate constants of $1x10^7$ $M^{-1}s^{-1}$, but removal is still less than 10%. For a $k_{M,HO}$ of $1x10^8$ $M^{-1}s^{-1}$, removal approaches 30%. Significant improvement in removal occurs for the rate constant of $1x10^9$ $M^{-1}s^{-1}$, and then additional improvement for $1x10^{10}$ $M^{-1}s^{-1}$. Since most organic compounds have rate constants, $k_{M,HO}$, in the range of $1x10^9$ to $1x10^{10}$ $M^{-1}s^{-1}$, these results indicate that treatment under these baseline conditions should yield removals in the range of 85-99% respectively.

Figure 10: Effect of Rate Constant of Micropollutant, M, with Hydroxyl Radical, HO

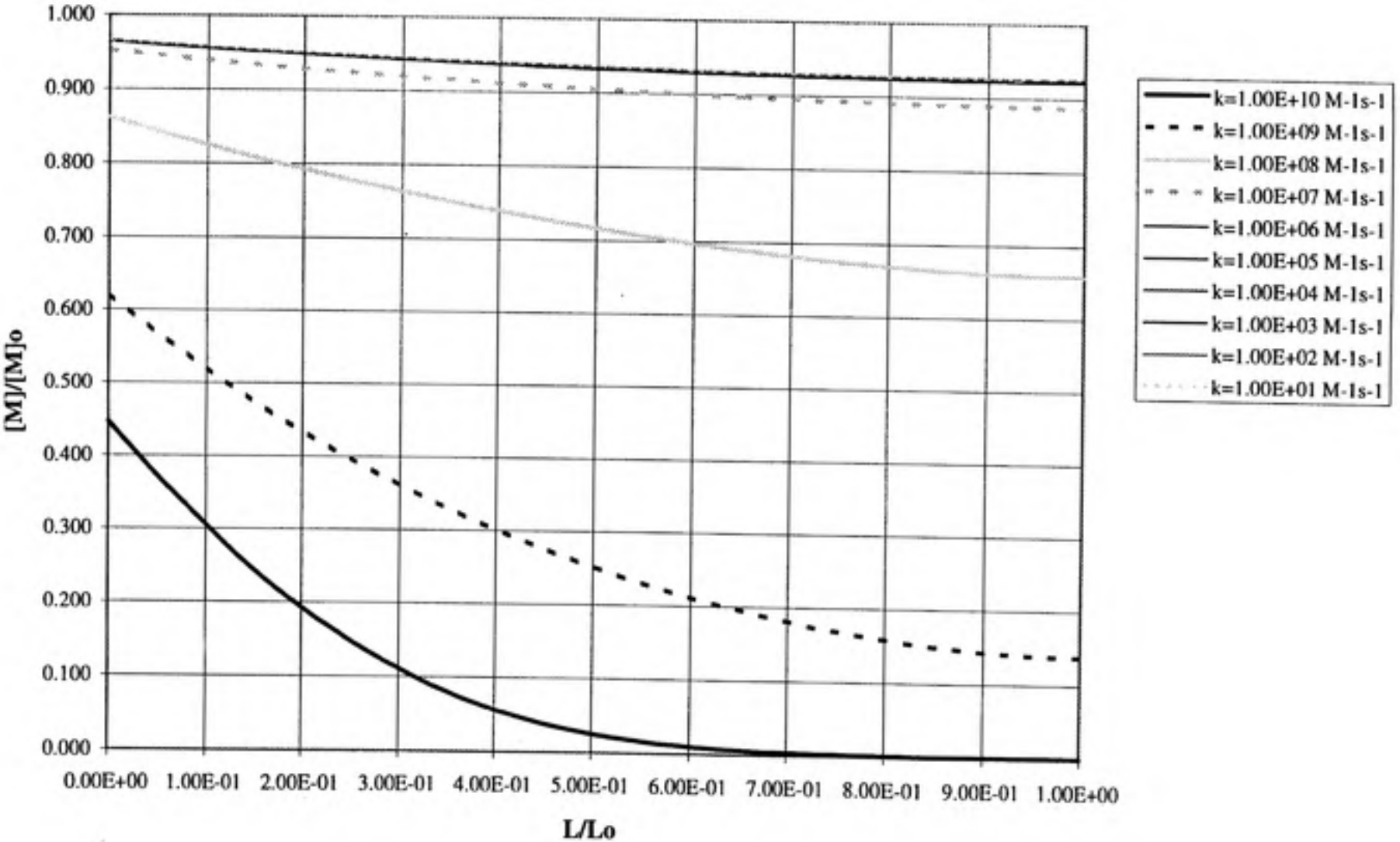

4.1.3 Mass Transfer Coefficient

Model runs were made varying mass transfer coefficients from 0.001 to 0.5 s^{-1}, bracketing the value (0.005 s^{-1}) which appears to describe the LADWP reactor (see Section 4.2, page 57). Results for micropollutant oxidation are shown in Figure 11. As previously mentioned, the reactions involving the O_3/H_2O_2 mechanism are very fast and can be mass transfer limited. The model predictions shown in Figure 11 reflect this mass transfer limitation for the lowest mass transfer coefficient. Increasing the mass transfer coefficient from 0.001 to 0.01 s^{-1} significantly improves the micropollutant destruction. For the next increases in k_La, the model predicts that the final % reduction approaches a constant value, reflecting a system no longer mass transfer limited, where micropollutant removal is a function of the rate of reaction.

Figure 11: Effect of Overall Mass Transfer Coefficient on Micropollutant Removal

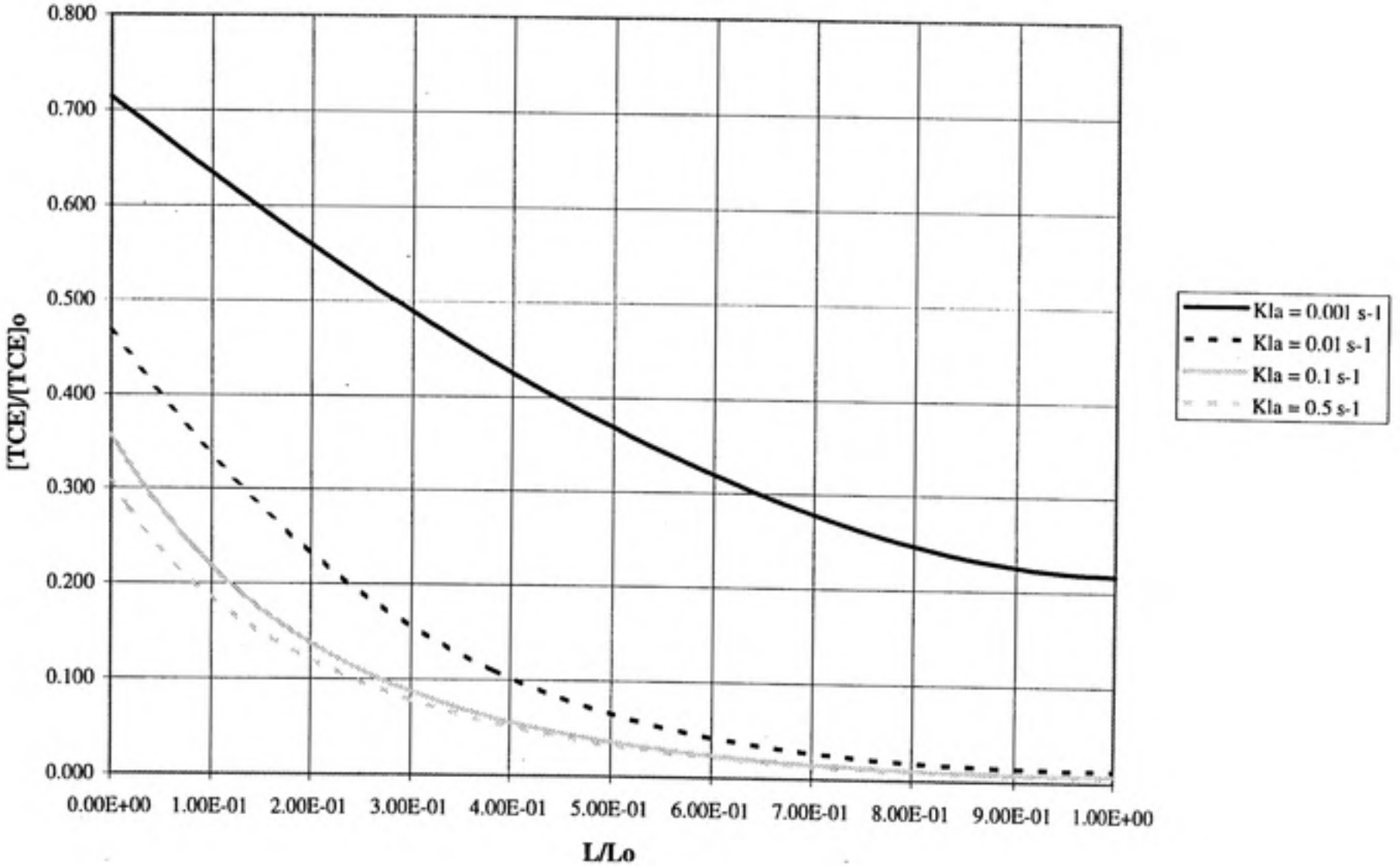

4.1.4 Liquid Phase Dispersion

Trials were run varying the liquid phase dispersion coefficient, D_L, over four orders of magnitude, as shown in Figure 12. The concentration profiles for TCE indicate that these trials encompass reactor performance which is nearly plug flow, D_L=0.001 m^2/s, to performance which is essentially completely mixed, D_L=1.0 m^2/s. The results indicate an increased micropollutant removal for decreasing dispersion, which nicely matches the accepted principal that plug flow reactors exhibit superior performance to completely mixed reactors. Comparing the results from Figure 12 to the LADWP data presented in Figure 18 indicates that the LADWP contactors have liquid phase dispersion coefficients in the range of 0.01 to 0.1 m^2/s.

Figure 12: Effect of Liquid Phase Dispersion Coefficient on Micropollutant Removal

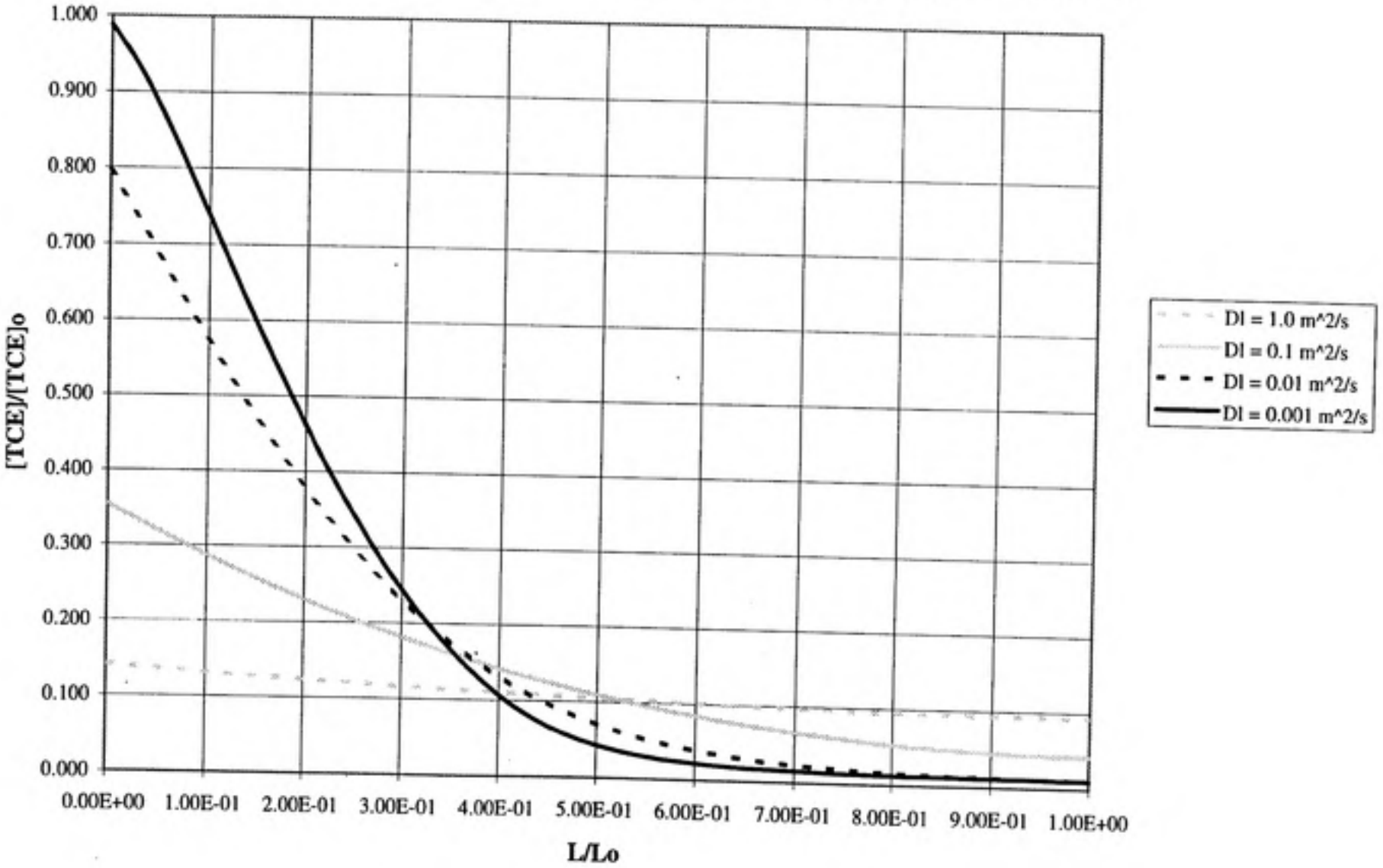

4.1.5 Gas Phase Dispersion

Gas phase dispersion is generally higher than dispersion in the liquid phase (Kago et al., 1989), and trial values for the gas phase dispersion coefficient, D_G, were run accordingly ranging from 0.01 to 5.0 m^2/s. These results are summarized in Figure 13. The lowest D_G shows the highest removal of TCE. Trials run for higher D_G values show a slight decrease in micropollutant destruction, and indicate that as the gas phase becomes completely mixed the removal rate decreases. Over the two orders of magnitude tested, the dispersion coefficient shows relatively little influence on the micropollutant removal compared to other parameters.

Figure 13: Effect of Gas Phase Dispersion Coefficient on Micropollutant Removal

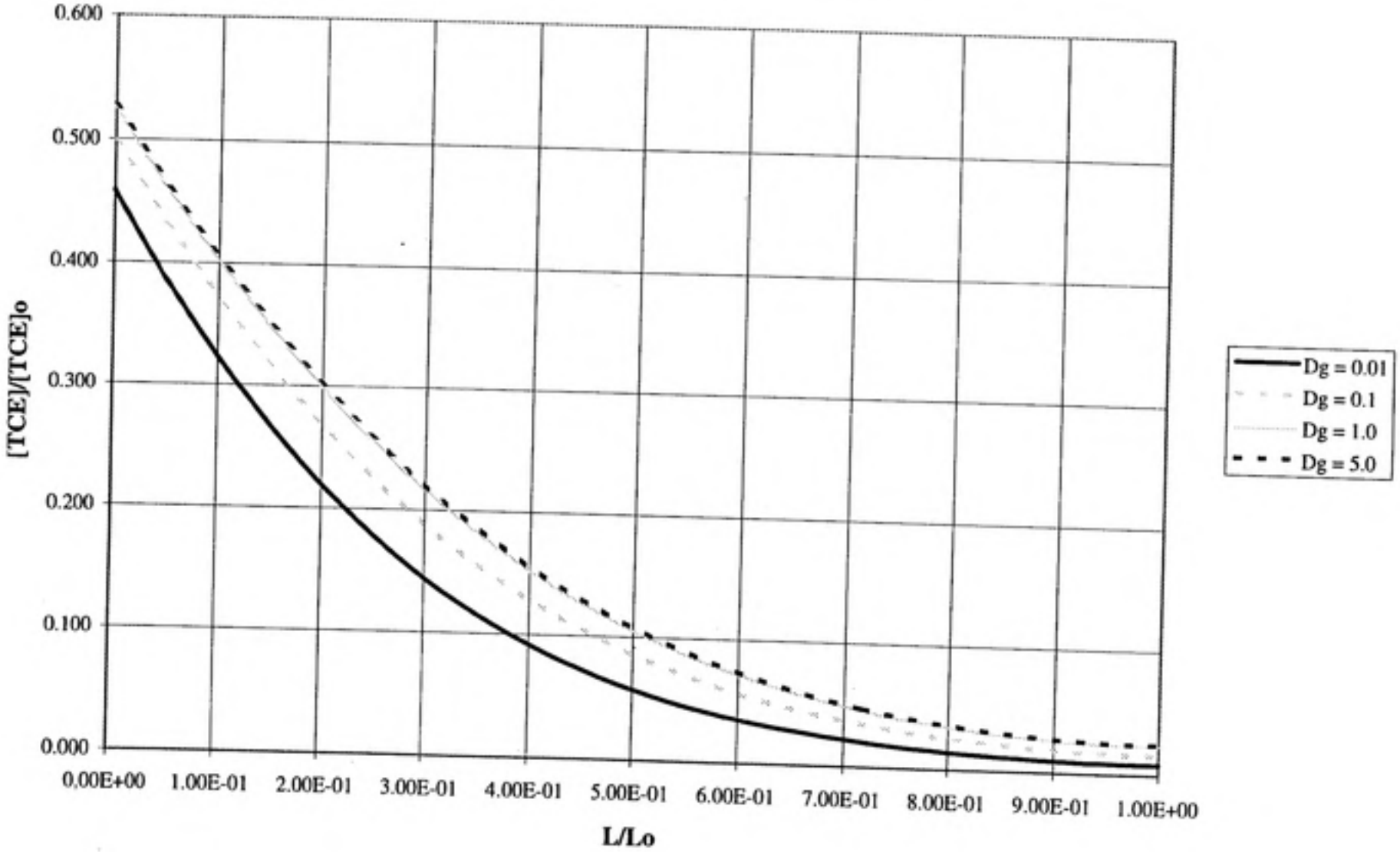

4.1.6 Carbonate Level

The bicarbonate and carbonate ions influence the O_3/H_2O_2 system because of the $HO^{\cdot}$ scavenging capabilities of these species. Trials were run varying total carbonate concentration from zero to $2.0x10^{-3}$ M. For the zero carbonate trial, the pH was kept at 7.8. For the other three trials, the pH was adjusted according to a closed carbonate system, resulting in pH of 8.0, 8.3, and 8.3 for trials of $1.00x10^{-4}$ M, $1.00x10^{-3}$ M, and $2.00x10^{-3}$ M. In this pH range, 95-98% of the total carbonate is present as $HCO_3^{\cdot}$ ($k_{HCO_3^{\cdot},OH} = 8.5x10^6\ M^{-1}s^{-1}$) and 0.3-1.0% is present as $CO_3^{2\cdot}$ ($k_{CO_3^{2\cdot},OH} = 3.9x10^8\ M^{-1}s^{-1}$).

It was expected that micropollutant removal would decrease with increasing total carbonate species. As shown in Figure 14, the model predicts the best removal of TCE at low total carbonate values. Removal at the highest total carbonate level is poorest. The two middle concentrations are interesting because, although the model predicts lower removal for the higher of the two carbonate concentrations as expected, the higher carbonate concentration shows higher removal for the first 80% of the reactor length, after which the two lines cross. Total TCE removal at the effluent to the reactor is inversely proportional to total carbonate level.

The level of carbonate in the system also has a significant influence on the liquid phase O_3 concentration. The liquid phase O_3 concentration profiles for the carbonate trials are shown in Figure 15. Note that the liquid phase O_3 concentration for zero carbonate is less than $1x10^{-7}$ M, apparently reflecting the rapid utilization of ozone by the sequence of reactions involving O_3 and H_2O_2, which yield the propagating species HO_2 (Equation 11, Figure 5). The highest O_3 residual occurs for the low carbonate concentration, a two

order of magnitude increase from the zero carbonate results. The inverse dependence of O_3 liquid phase concentration on the three different levels of total carbonate is counter intuitive to those familiar with ozone residuals in the absence of H_2O_2, where high levels of carbonate stabilize O_3. The O_3/H_2O_2 system differs from the O_3-only system in that the radical ion $CO_3^{\cdot}$ reacts primarily with H_2O_2 and its conjugate base (as shown in Equations 15 and 16, Figure 5) producing HO_2 and $O_2^{\cdot}$ respectively, both of which consume O_3. This influence of carbonate is of interest in terms of meeting CT requirements for disinfection, and the interplay of H_2O_2 and carbonate effects are probably not well appreciated by the water industry.

Figure 14: Effect of Total Carbonate Concentration on Micropollutant Removal

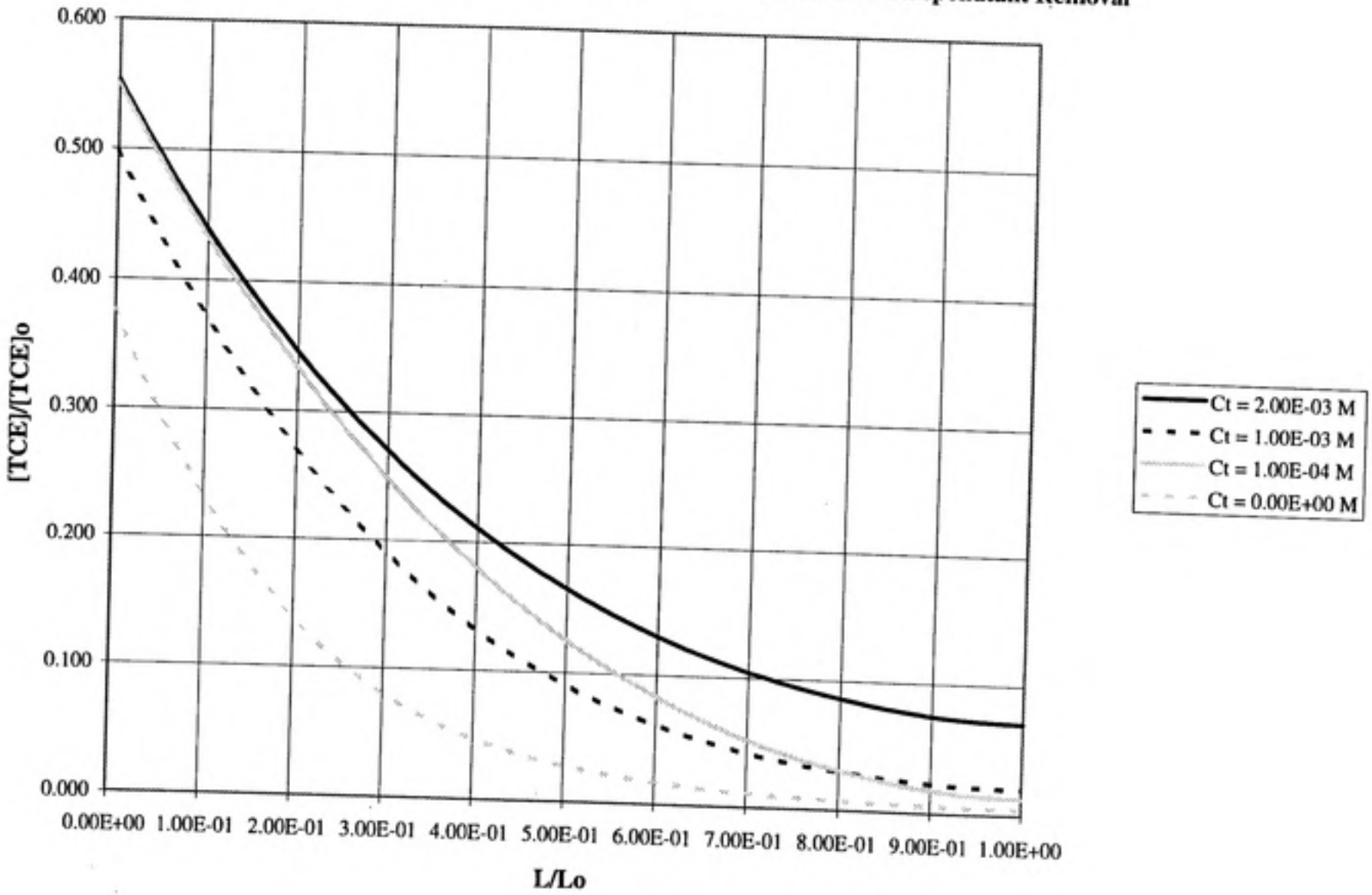

Figure 15: Effect of Total Carbonate Concentration on Liquid Phase Ozone Concentration

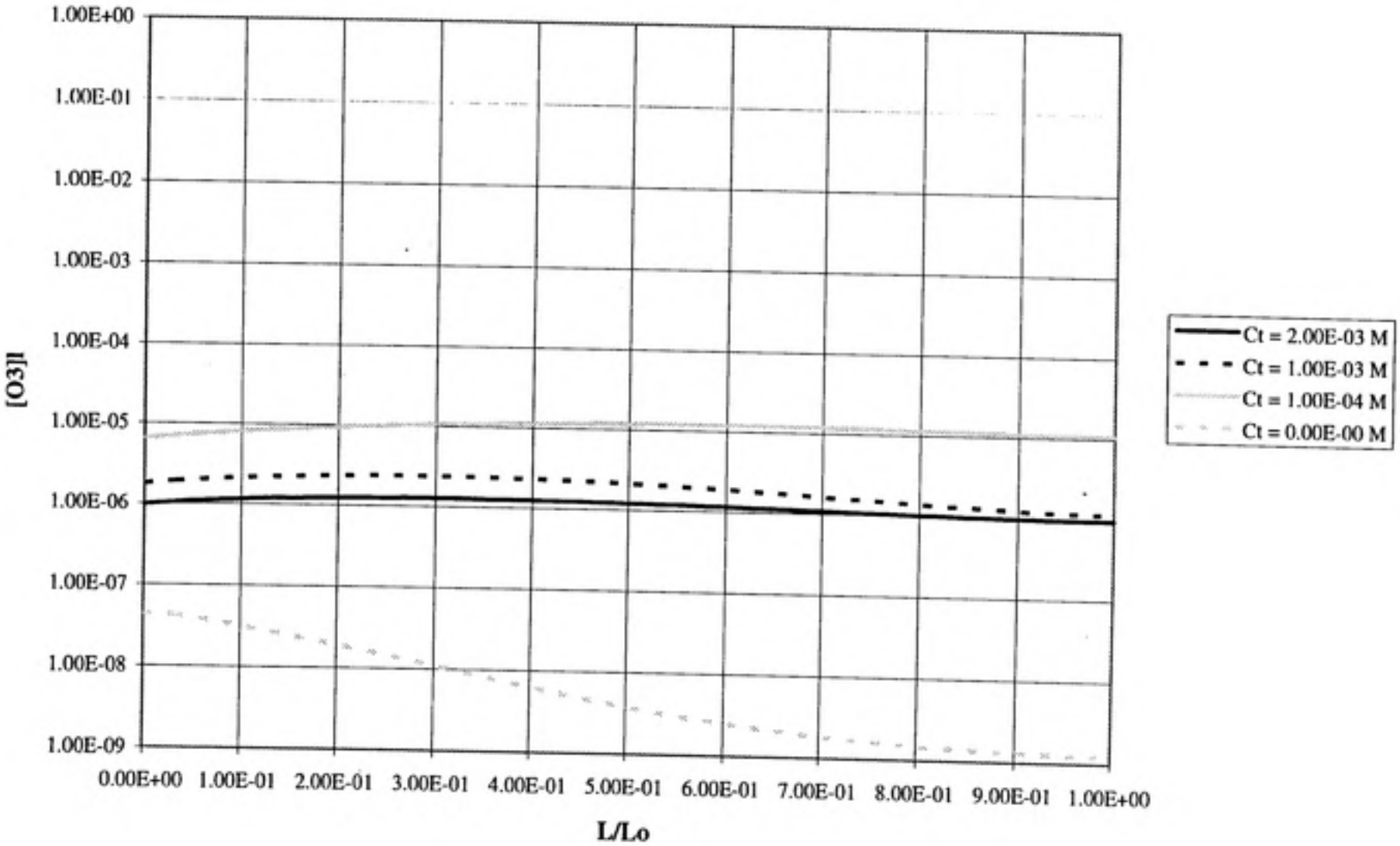

4.1.7 Influent pH

Trials run for a wide range of influent pHs are summarized in Figure 16. The influent pH plays a significant role in the removal of a micropollutant for several reasons. As the pH increases, the decomposition of O_3 can be initiated by the increasing concentrations of OH^- and the conjugate base of H_2O_2 ($pK_a = 11.8$). However, in a system with carbonate species present, as the system pH approaches 10.3, the pKa_2 for H_2CO_3, the inorganic carbon will be converted to carbonate ion, the carbonate species with the highest rate constant with $HO^{\cdot}$. This significantly increases the scavenger effects, and should decrease micropollutant removal. Model predictions shown in Figure 16 clearly demonstrate this effect. The model predicts increasing removal as the pH moves from 5.0 to 9.0, with the most significant increase occurring between pH 5.0 and 7.0. Then at pH 10, the model predicts a significant drop in removal compared to that at pH 9.0, which can be attributed to the increasing concentration of CO_3^{2-}.

Figure 16: Effect of Influent pH on Micropollutant Removal

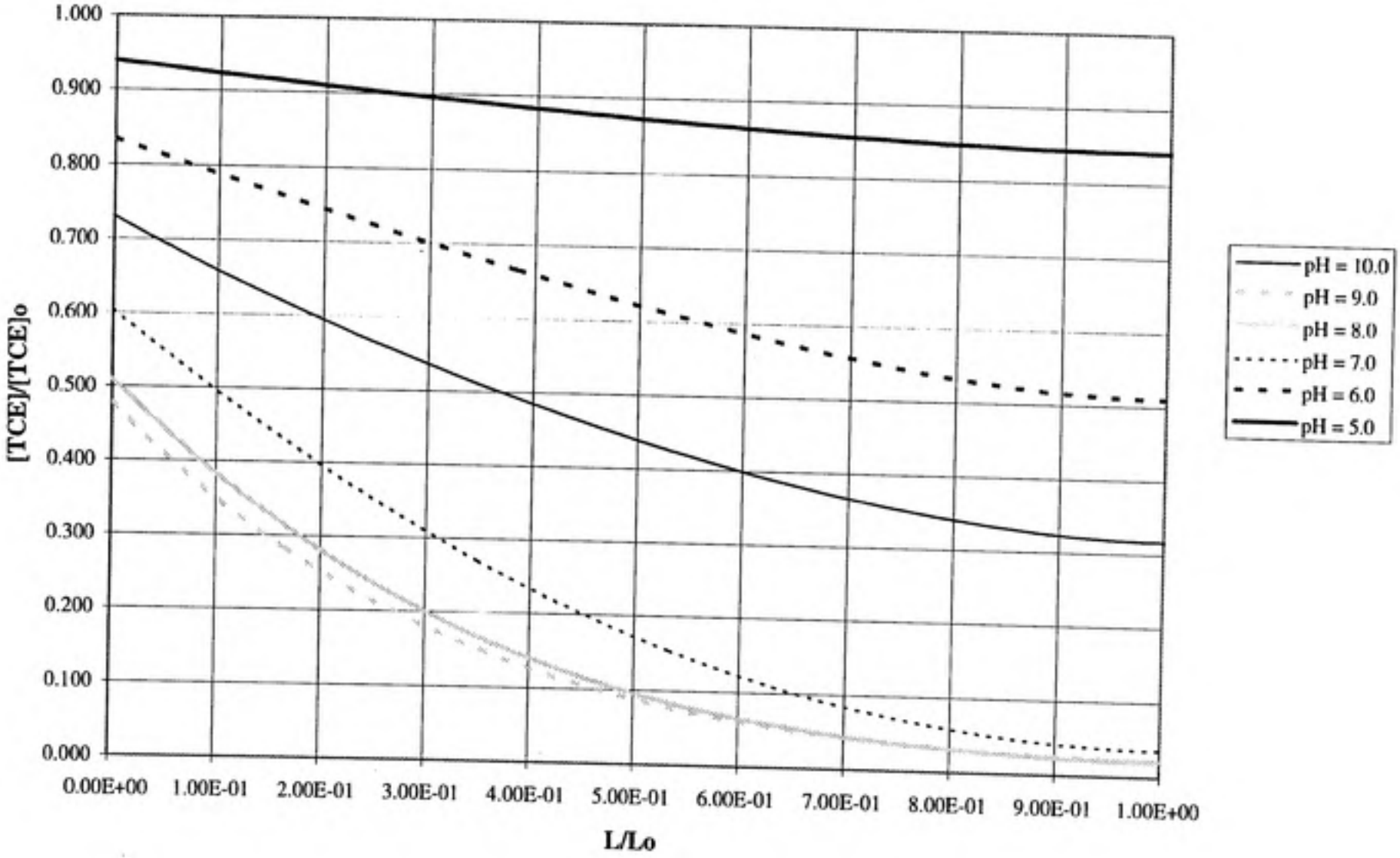

4.1.8 Reactor Configuration

Bubble contactors can be run co-current or counter-current. Model results shown in Figure 17 for the two different configurations under otherwise identical conditions do not predict a significant performance advantage for one reactor configuration over the other. Although one might expect that the counter-current contactor would have a better performance due to a high mass transfer driving force (the difference between the liquid and gas phase concentrations), the model does not show this effect. This may be a reflection of the high rate of chemistry, particularly at the influent of the co-current reactor. Under the specified conditions, the system is operating in a range where the micropollutant destruction is mass transfer limited and O_3 is decomposing rapidly in the liquid phase. As a result of the relatively low O_3 liquid phase concentration, the reactor configuration does little to increase the mass transfer driving force.

Figure 17: Counter Current vs Co-Current Contactor Performance

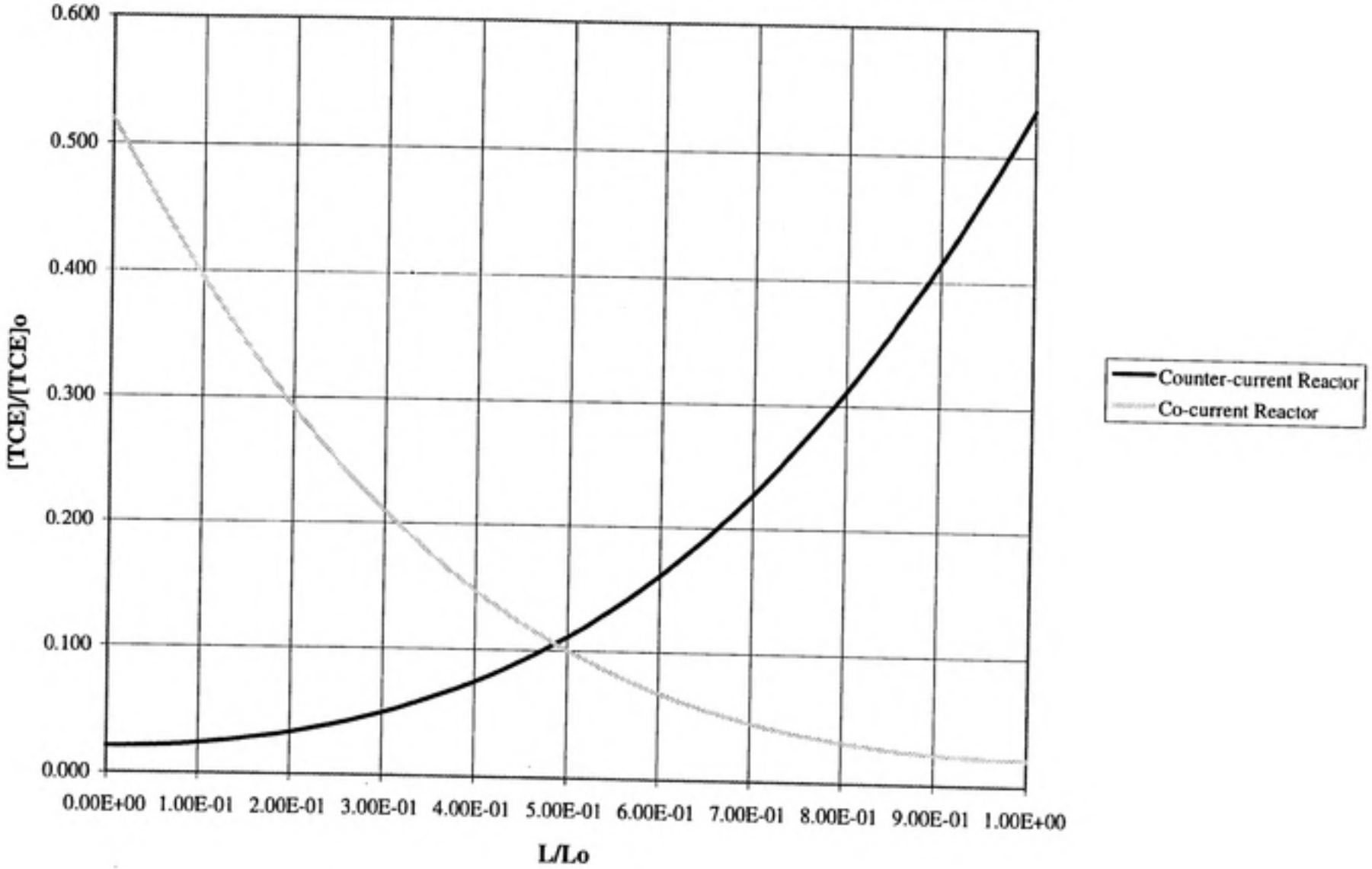

4.2 *Los Angeles Department of Water and Power Ozone/Peroxide Plant*

The data provided by LADWP personnel included micropollutant concentration profiles in the first of the two contactors for one set of operating conditions. Although not all model input parameters were available, it was decided that a preliminary comparison between the profile data and model predictions would be instructive. The flow rates for liquid and gas phases were provided, as were contactor dimensions and influent concentrations. Tracer test data characterizing the mixing conditions in the reactor were unavailable, so the mass transfer coefficient and the dispersion coefficients for the liquid and gas phases were estimated using empirical correlations from the chemical engineering literature. The references, predicted values, and the actual inputs are shown in Table 4. The mass transfer coefficient was multiplied by the volume fraction of water to account for differences in governing equations.

Table 4: Estimated Parameters For LADWP Input File

Parameter	Reference	Empirical Value	Adjusted Value
D_G	Wachi and Nojima, 1990	4.0×10^{-1} m^2/s	-
D_L	Deckwer et al., 1974	4.0×10^{-2} m^2/s	-
k_La	Deckwer et al., 1983	2.5×10^{-3} s^{-1}	5.0×10^{-3} s^{-1}

Preliminary model results indicated that the estimated mass transfer coefficient was under predicting transfer of O_3. When the k_La was increased by a factor of two, the model predictions for both TCE and PCE were significantly improved. These results are shown in Figure 18. The model prediction for TCE removal appears better than that for PCE removal.

Figure 18: LADWP Profile Data and Model Prediction

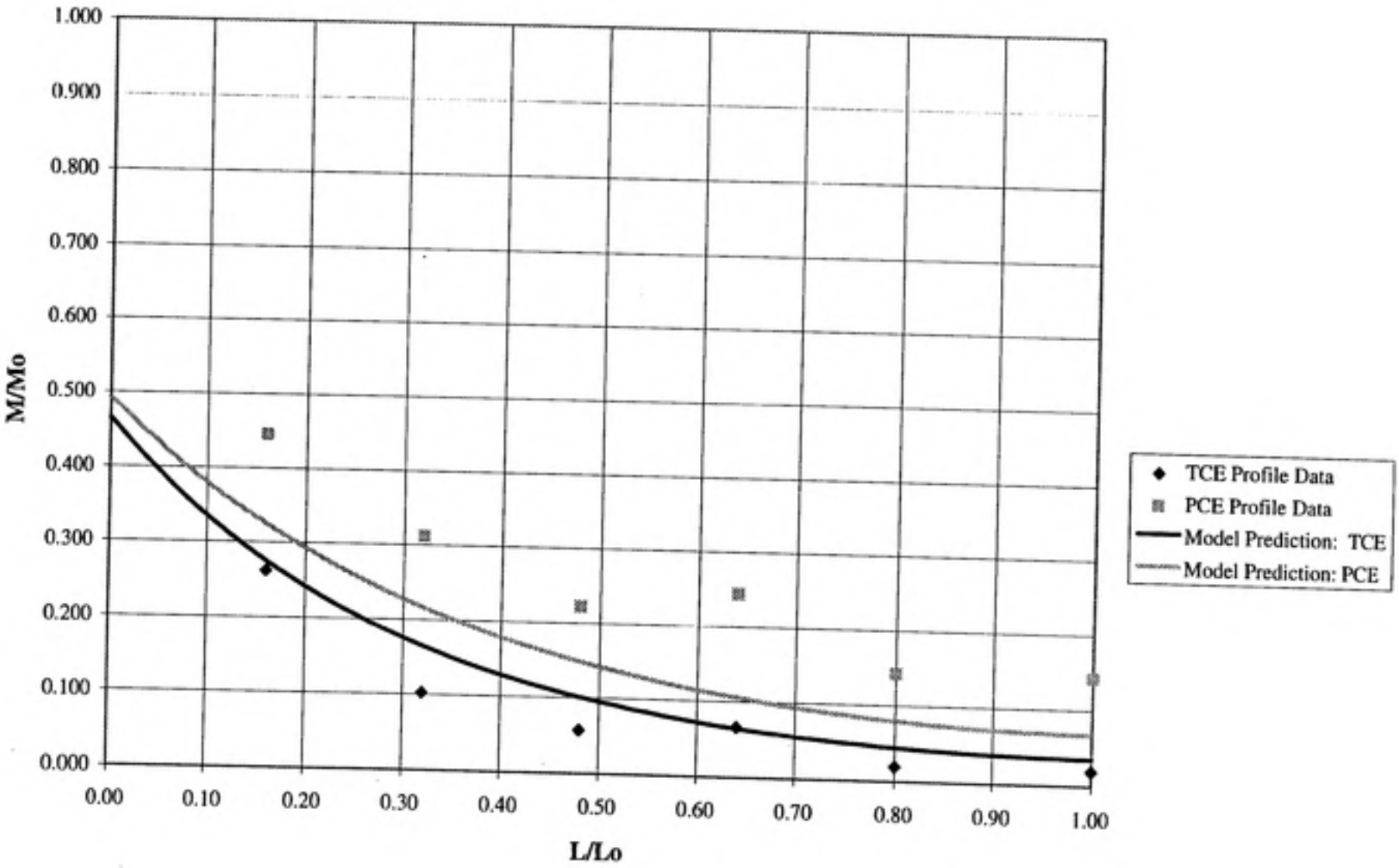

5. CONCLUSIONS

Under the specified conditions for this work, the model results indicate that D_L and k_La are very important parameters both in modeling and optimizing the O_3/H_2O_2 system removal of a micropollutant. Rate constants between specific micropollutants and influent concentrations will primarily be a function of the specific design goal and will not be parameters that will lend themselves to design adjustment. The gas phase dispersion and the reactor configuration (co-current or counter current) have less significant effects on the micropollutant destruction.

The results presented are a function of 17 different rate constants, several Henry's constants, dispersion coefficients and mass transfer coefficients. The results will always reflect the accuracy and detail of the input file. The present input file does not include by-products for the degradation of TCE. In the case of TCE and other similar micropollutants which apparently yield rapid mineralization after initial $HO^{\cdot}$ attack, this will not severely influence the predictions for the O_3/H_2O_2 system. However, in other cases lack of such information may influence the accuracy of model predictions. Even so, the model is a useful tool for exploring the response of this system to varying conditions and can be used to predict the applicability of AOPs to specific waste streams.

The original intent was to develop a model that could be run on a desk top IBM compatible computer, so that most potential users would have the capabilities to run the model themselves. The present version requires significantly more memory to run and to run quickly and is presently run on a Hewlett Packard Apollo workstation. The transient predictions of the model are very valuable in terms of predicting the response of the

O_3/H_2O_2 system, but the development of a simpler steady state model would require less memory. Such a model would not have the ability to predict how long it would take a system to reach steady state after conditions change, but would fit well into the goals of the Technology Assessment Project in providing first cut evaluations of AOP applicability.

REFERENCES

Aieta, E. Marco, Kevin M. Reagan, John S. Lang, et al. "Advanced Oxidation Processes for Treating Groundwater Contaminated with TCE and PCE: Pilot-Scale Evaluations." *Journal AWWA* May 1988. 64-72.

Behar, D., G. Czapski, and I. Duchovny. "Carbonate Radical in Flash Photolysis and Pulse Radiolysis of Aqueous Carbonate Solutions." *J. Phys. Chem.* 74(10) 1970. 2206.

Bielski, B. H. J., D. E. Cabelli, R. L. Arudi, et al. "Reactivity of HO2/O2- Radicals in Aqueous Solution." *J. Phys. Chem. Ref. Data* 14 1985. 1041.

Braun, Walter, John T. Herron, and David K. Kahaner. "Acuchem: A Computer Program for Modeling Complex Chemical Reaction Systems." *International Journal of Chemical Kinetics* 20 1988. 51-62.

Brodard, E., P. Kassem, M. Roustan, et al. "Basic Concepts in Ozone Contactor Design." Proceedings from AWWA National Conference. Kansas City, 14 June 1987. : AWWA.

Buler, R. E., J. Staehelin, and J. Hoigne. "Ozone Decomposition in Water Studied by Pulse Radiolysis 1. HO2/O2 and HO3/O3 as Intermediates." *J. Phys. Chem.* 88 1984. 2560.

Buxton, G. V., C. L. Greenstock, W. P. Helman, et al. "Critical Review of Rate Constants for Reactions of Hydrated Electrons, Hydrogen Atoms and Hydroxyl Radicals in Aqueous Solution." *J. Phys. Chem. Ref. Data* 17 1988. 513-886.

Christensen, H. S., H. Sehested, and H. Corfitzan. "Reactions of Hydroxyl Radicals with Hydrogen Peroxide at Ambient and Elevated Temperatures." *J. Phys. Chem.* 86 1984. 15-88.

Petzold, Linda. DDASSL.FOR. Computer software. 1983.

Decker, W. D., R. Burckhart, and G. Zoll. "Mixing and Mass Transfer in Tall Bubble Columns." *Chemical Engineering Science* 29 1974. 2177-2188.

Deckwer, W. D., K. Nguyen-Tien, B. G. Kelkar, et al. "Applicability of Axial Dispersion Model to Analyze Mass Transfer Measurements in Bubble Columns." *AIChE Journal* 29(6) Nov. 1983. 915-922.

Field, R. J., N. V. Raghavan, and J. G. Brummer. "A Pulse Radiolysis Investigation of the Reactions of BrO2 radical with Fe(CN)6(4-), Mn(II), phenoxide ion and phenol." *J. Phys Chem* 86 1982. 2443-9.

Getoff, N. "Radiation and Photoinduced Degradation of Pollutants in Water. A Comparative Study." *Radiat. Phys. Chem.* 37 1991. 673-80.

Glaze, W. H., Joon-Wun Kang, and Douglas Chapin. "The Chemistry of Water Treatment Processes Involving Ozone, Hydrogen Peroxide, and Ultraviolet Radiation." *Ozone Science and Engineering* 9 1987. 335-352.

Glaze, W. H., and G. R. Peyton. "Mechanism of Photolytic Ozonation." Photochemistry of Environmental Aquatic Systems. R. G. Zika, and W. J. Cooper. ACS Symposium Series No. 327 . Washington D.C.: American Chemical Society, 1987. 76-88.

Glaze, William H. "An Overview of Advanced Oxidation Processes: Current Status and Kinetic Models." Proceedings of The Third International Symposium Chemical Oxidation: Technology for the Nineties. , 17 Feb. 1993.

Glaze, William H., Chairman, Environmental Sciences and Engineering. "A Summary of the Working Group on Ozonation and Combined Methods." First International EPRI/NSF Symposium on Advanced Oxidation. San Francisco, CA, 22 Feb. 1993. Albany, CA: CK & Associates.

Glaze, William H., and Joon-Wun Kang. "Advanced Oxidation Processes. Test of a Kinetic Model for the Oxidation of Organic Compounds with Ozone and Hydrogen Peroxide in a Semibatch Reactor." *Ind. Eng. Chem. Res.* 28(11) Nov. 1989b. 1580-1587.

Glaze, William H., and Joon-Wun Kang. "Advanced Oxidation Processes. Description of a Kinetic Model for the Oxidation of Hazardous Materials in Aqueous Media with Ozone and Hydrogen Peroxide in a Semibatch Reactor." *Ind. Eng. Chem. Res.* 28(11) Nov. 1989a. 1573-1580.

Glaze, William H., Raymond Schep, William Chauncey, et al. "Evaluating Oxidants for the Removal of Model Taste and Odor Compounds From a Municipal Water Supply." *Journal of AWWA* May 1990. 79-84.

Glaze, Wm. H., Susan Homewood, and Kathryn Iwamasa. Assessment of Industrial Wastewater Treatment Technologies: Annual Report 1994. University of North Carolina, Dec. 1994.

Haas, Charles N., and Richard J. Vamos. Hazardous and Industrial Waste Treatment. Englewood Cliffs, New Jersey: Prentice-Hall, 1995.

Hoigne, J. "Mechanisms, Rates and Selectivities of Oxidations of Organic Compounds Initiated by Ozonation of Water." Ozone Technology and its Practical Applications Volume I. Ann Arbor, MI: Ann Arbor Science, 1982. 341-379.

Hoigne, J., and H. Bader. "Ozonation of Water: Role of Hydroxyl Radicals as Oxidizing Intermediates." *Science* 190 1975. 782-784.

Hoigne, J., and H. Bader. "Rate Constants of Reaction of Ozone with Organic and Inorganic Compounds in Water:I Non-dissociating Organic Compounds." *Water Res.* 17 1983. 173-183.

Hoigne, J., and H. Bader. "Rate Constants of Reaction of Ozone with Organic and Inorganic Compounds in Water:II Dissociating Organic Compounds." *Water Res.* 17 1983. 185-194.

Hoigne, J., and H. Bader. "The Role of Hydroxyl Radical Reactions in Ozonation Processes in Aqueous Solutions." *Water Research* 10 1976. 377-386.

Hull, Chris. [Personal Communication with Kerry Kelly]. University of North Carolina, Feb. 1991.

Hull, Christopher S., Philip C. Singer, K. Saravanan, et al. "Ozone Mass Transfer and Reaction: Completely Mixed Systems." Annual AWWA Conference: Water Quality. Vancouver. , 1992. 457-465.

Jeffries, Harvey, Micheal Gery, and Kathy Murphy. Advanced Chemical Reaction Mechanisms and Solvers for Models-3: Progress Report. University of North Carolina, Chapel Hill, NC, 15 Sept. 1993.

Kago, T., Y. Sasaki, T. Kondo, et al. "Gas Holdup and Axial Dispersion of Gas and Liquid in Bubble Columns of Homogeneous Bubble Flow Regime." *Chem. Eng. Comm.* 75 1989. 23-28.

Karimi, Ali. [Personal Communication]. Los Angeles Department of Water and Power, Sept. 1995.

Kelly, Kerry. Investigation of Ozone Induced PCE Decomposition in Natural Waters. Thesis, Chapel Hill, NC: University of North Carolina-Chapel Hill, 1991.

Kochany, J., and J. R. Bolton. "Mechanism of Photo Degradation of Aqueous Organic Pollutants 2. Measurement of the primary rate constants for reaction of OH radicals with benzene and some halobenzenes using an PER spin trapping method following the photolysis of H2O2." *Environmental Science and Technology* 26 1992. 262-5.

Laplanche, A., M. T. Orta De Velasquez, V. Boisdon, et al. "Modelisation of Micropollutant Removal in Drinking Water Treatment by Ozonation or Advanced Oxidation Processes (O3/H2O2)." *Ozone Science and Engineering* 17 1995. 97-117.

Le Sauze, N., A. Laplanche, M. T. Orta De Velasquez, et al. "The Residence Time Distribution of the Liquid Phase In a Bubble Column and Its Effect on Ozone Transfer." *Ozone Science & Engineering* 14 1992. 245-262.

Marinas, Benito J., Sun Liang, and E. Marco Aieta. "Modeling Hydrodynamics and Ozone Residual Distribution in a Pilot-Scale Ozone Bubble-Diffuser Contactor." *Journal of AWWA* Mar. 1993. 90-99.

Miller, C. T., "ENVR 281: Advanced Numerical Modeling." Class Lecture Notes, University of North Carolina-Chapel Hill, 1995.

Parker, J. C., and M. Th. van Genuchten. Determining Transport Parameters from Laboratory and Field Tracer Experiments. Blackburg, VA: Virginia Agriculture Experiment Station, Virginia Polytechnic Institute and State University, May 1984.

Pedit, Joseph A. [Personal Communication]. University of North Carolina, Sept. 1995.

Peyton, G. R., and W. H. Glaze. "Destruction of Pollutants in Water with Ozone in Combination with Ultraviolet Radiation. 3. Photolysis of Aqueous Ozone." *Environmental Science and Technology* 22 1988. 761.

Peyton, Gary R., and Chai S. Gee. Aquatic Humic Substances: Influence on Fate and Treatment of Pollutants. Catalytic Competition Effects of Humic Substances on Photolytic Ozonation of Organic Compounds. : American Chemical Society, 1989.

Rice, Rip G. [Personal Communication]. 3 May 1995.

Rice, Rip G., and Aharon Netzer. Handbook of Ozone Technology and Applications: Volume I. Ann Arbor, MI: Ann Arbor Science Publishers, 1982.

Snoeyink, Vernon L., and David Jenkins. Water Chemistry. New York: John Wiley and Sons, Inc., 1980.

Staehelin, Johannes, and Jurg Hoigne. "Decomposition of Ozone in Water: Rate of Initiation by Hydroxide Ions and Hydrogen Peroxide." *Environmental Science and Technology* 16(10) 1982. 676-681.

Staehelin, Johannes, and Jurg Hoigne. "Decomposition of Ozone in Water in the Presence of Organic Solutes Acting as Promoters and Inhibitors of Radical Chain Reactions." *Environmental Science and Technology* 19(12) 1985. 1206-1213.

Stumm, Werner, and James J. Morgan. Aquatic Chemistry: An Introduction Emphasizing Chemical Equilibria in Natural Waters. New York: Wiley-Interscience, 1970.

Taube, T. "Photochemical Reactions of Ozone in Solution." *Trans. Faraday Soc.* 53 1957. 656.

Wachi, Shun, and Yasuhiro Nojima. "Gas-Phase Dispersion in Bubble Columns." *Chemical Engineering Science* 45(4) 1990. 901-905.

Yao, C. C. D., and W. R. Haag. "Rate Constants for Direct Reactions of Ozone with Several Drinking Water Contaminants." *Water Res.* 25 1991. 761-73.

Yurteri, Coskun. Removal of Organic Pollutants By Ozonation: Kinetic and Reactor Design. Dissertation: Drexel University, 1991.

APPENDIX A: Example Input File

```
 1.00000E-10 1.00000E-12                                  ------Num. Method----
  30   2  10
 3.80000E-00 6.92500E+00                                  ------Reactor Info---
 0.66300E+00 0.13700E+00
 0.13500E-00 0.02760E-00
 0.04000E+00 4.00000E-01
  15                                                       ------Species-----
H2O2            1   0 0.00000E+00 0.00000E+00
H02-            1   0 0.00000E+00 0.00000E+00
H+              1   0 0.00000E+00 0.00000E+00
03              1   1 3.71000E+00 5.00000E-03
03-             1   0 0.00000E+00 0.00000E+00
HO2             1   0 0.00000E+00 0.00000E+00
OH-             1   0 0.00000E+00 0.00000E+00
O2-             1   0 0.00000E+00 0.00000E+00
HO3             1   0 0.00000E+00 0.00000E+00
OH              1   0 0.00000E+00 0.00000E+00
TCE             1   1 4.10000E-01 5.00000E-03
HCO3-           1   0 0.00000E+00 0.00000E+00
CO3-            1   0 0.00000E+00 0.00000E+00
CO3--           1   0 0.00000E+00 0.00000E+00
H2CO3* / CO2    1   1 1.00000E-01 5.00000E-03
  17                                                     ------Reactions----
   1 5.50000E+06   2   4   0   5   6   0  1.  1.  0.  1.  1.  0.
   1 70.0000E+00   7   4   0   8   6   0  1.  1.  0.  1.  1.  0.
   1 1.60000E+09   8   4   0   5   0   0  1.  1.  0.  1.  0.  0.
   1 5.20000E+10   5   3   0   9   0   0  1.  1.  0.  1.  0.  0.
   1 1.10000E+05   9   0   0  10   0   0  1.  0.  0.  1.  0.  0.
   1 15.0000E+00  11   4   0   0   0   0  1.  1.  0.  0.  0.  0.
   1 2.90000E+09  10  11   0   0   0   0  1.  1.  0.  0.  0.  0.
   1 7.50000E+09  10   2   0   7   6   0  1.  1.  0.  1.  1.  0.
   1 2.70000E+07  10   1   0   6   0   0  1.  1.  0.  1.  0.  0.
   1 8.50000E+06  10  12   0  13   0   0  1.  1.  0.  1.  0.  0.
   1 3.90000E+08  10  14   0   7  13   0  1.  1.  0.  1.  1.  0.
   1 1.10000E+08  10   4   0   6   0   0  1.  1.  0.  1.  0.  0.
   1 8.00000E+05  13   1   0   6  12   0  1.  1.  0.  1.  1.  0.
   1 5.60000E+07  13   2   0   8  12   0  1.  1.  0.  1.  1.  0.
   1 8.30000E+05   6   0   0   1   0   0  2.  0.  0.  1.  0.  0.
   1 9.70000E+07   8   6   0   1   7   0  1.  1.  0.  1.  1.  0.
   1 2.20000E+06  13   0   0   0   0   0  2.  0.  0.  0.  0.  0.
   5
1.58489E-12   1   0   0   2   3   0  1.  0.  0.  1.  1.  0.
1.58489E-05   6   0   0   8   3   0  1.  0.  0.  1.  1.  0.
5.01187E-07  15   0   0   3  12   0  1.  0.  0.  1.  1.  0.
5.01187E-11  12   0   0   3  14   0  1.  0.  0.  1.  1.  0.
1.00000E-14   0   0   0   3   7   0  0.  0.  0.  1.  1.  0.
  1
  5 1.00000E+03
  1
  3   7   5
7.80000E+00 7.80000E+00
  9
  2   1   2   1                      ----------Initial Conditions---------
0.00000E-00 7.06000E-05
  2   6   8   2
0.00000E-00 0.00000E-00
  3  15  12  14   3   4
1.00000E-03 1.00000E-03
  1   4
0.00000E-00 0.00000E-00
```

```
  1   5
0.00000E-00 0.00000E-00
  1   9
0.00000E-00 0.00000E-00
  1  10
0.00000E-00 0.00000E-00
  1  11
7.64000E-06 7.64000E-06
  1  13
0.00000E-00 0.00000E-00
  3
  4
0.00000E-04 3.50000E-04
 11
0.00000E-00 0.00000E-00
 15
0.00000E-00 0.00000E-00
  1
 17                              ---------Output-----------
  1   1
  2   1
  3   1
  4   1
  4   2
  6   1
  7   1
  8   1
  9   1
 10   1
 11   1
 11   2
 12   1
 13   1
 14   1
 15   1
 15   2
```